

Video Transformers: A Survey

Javier Selva^{1,3}, Anders S. Johansen², Sergio Escalera^{1,2,3},
Kamal Nasrollahi^{2,4}, Thomas B. Moeslund², Albert Clapés^{2,3}

¹Universitat de Barcelona ²Aalborg University ³Computer Vision Center ⁴Milestone Systems
jselvaca21@alumnes.ub.edu, {alcl,asjo,kn,tbm}@create.aau.dk, sergio@maia.ub.es

Abstract—Transformer models have shown great success modeling long-range interactions. Nevertheless, they scale quadratically with input length and lack inductive biases. These limitations can be further exacerbated when dealing with the high dimensionality of video. Proper modeling of video, which can span from seconds to hours, requires handling long-range interactions. This makes Transformers a promising tool for solving video related tasks, but some adaptations are required. While there are previous works that study the advances of Transformers for vision tasks, there is none that focus on in-depth analysis of video-specific designs. In this survey we analyse and summarize the main contributions and trends for adapting Transformers to model video data. Specifically, we delve into how videos are embedded and tokenized, finding a very widespread use of large CNN backbones to reduce dimensionality and a predominance of patches and frames as tokens. Furthermore, we study how the Transformer layer has been tweaked to handle longer sequences, generally by reducing the number of tokens in single attention operation. Also, we analyse the self-supervised losses used to train Video Transformers, which to date are mostly constrained to contrastive approaches. Finally, we explore how other modalities are integrated with video and conduct a performance comparison on the most common benchmark for Video Transformers (i.e., action classification), finding them to outperform 3D CNN counterparts with equivalent FLOPs and no significant parameter increase.

Index Terms—Artificial Intelligence, Computer Vision, Self-Attention, Transformers, Video Representations



1 INTRODUCTION

TRANSFORMERS are a recent family of models first proposed in [1]. Originally designed to replace recurrent layers in a machine translation setting, these architectures have seen a quick adoption for modeling many other data types [2], [3], [4], including images [5], [6], [7], [8] and videos [9], [10], [11], [12], [13], [14].

The key success behind Transformers is their non-local token mixing strategy through the self-attention (SA) operation. The non-local operation was proposed in [15] as a generalization of the non-local mean operation [16]. It evolves the input representation based on interactions among all its elements. These interactions are modulated through a pair-wise affinity function that weighs the contribution that every element should have on any other. Different from a fully connected (FC) layer a non-local operation needs no weights: the relationships between inputs is not learned, but entirely dependent on the input representations. Despite their success, the very nature of SA causes Transformers to scale poorly with sequence length T . In particular, the complexity of SA is $\mathcal{O}(T^2)$ due to the pair-wise affinity computation. Furthermore, Transformers lack any inductive biases, which may be a desirable property, but it can also hinder learning unless large quantities of data are used [7].

The recent surge in Transformer works makes it convoluted to keep track of the latest advances and trends. Recent surveys try to fill this gap by analysing and summarizing architectural design choices for Transformers in general [17], focusing on NLP [18], or on efficient designs, such as [19] or [20]. While some have extensively surveyed advances for visual, e.g. [21], [22], [23], [24] and Vision-Language Transformers [25], they miss an in-depth analysis

of video models. The survey in [26] focuses on pre-training for video and language Transformers, but while they discuss some architectural choices, they do not cover general video-only trends. *Video Transformers* (VTs) find commonalities with other Transformer designs (specially within the image domain), but the inherently large dimensionality of video will exacerbate Transformer limitations and require special treatment. The additional temporal dimension also calls for different embeddings, tokenization strategies, and architectures. Finally, video media is usually paired with other modalities (e.g., it is very naturally accompanied by audio), which makes it specially prone to be used in multi-modal settings.

1.1 Scope

Video. The focus of this work is to comprehensively analyze the recent advances of Transformer architectures for modeling video data. Note that works which employ traditional (non-Transformer) architectures to map videos into other structured form (e.g., joints [27] or speech [28]) before being modeled by the Transformer layers fall out of our scope. We are particularly interested in models that use (temporal) visual features as input to the SA layers. We analyze the manner in which the literature is adapting these models to be able to handle the inherent complexity of videos plus, optionally, other modalities. We do consider, however, works which leverage some CNN architecture to embed the video data into lower-dimensional space before using Transformer layers (see Sec. 3.1.1).

Transformers. As opposed to locality based architectures (such as CNNs), Transformers model global interactions of

the data at each layer. However, there is a wide spectrum of globality based architectures. We focus on works that use SA in the form of the Embedded Gaussian variant of the non-local operation [15] with additional normalization factor (see Eq. (1)). The literature has regarded other forms of attention as SA [29], [30], [31], [32], but these generally use FC layers instead of dot-product to compute attention weights. We consider these to be out of the scope of this survey. Furthermore, research directions concurrent to Transformers have also employed either SA or an equivalent Embedded Gaussian version of the non-local operator for Computer Vision tasks. For instance, Graph Attention Networks, as [33] and [34], or Relation Networks, such as [35] and [36]. Similarly, we also find them used to enhance CNN backbones, either by adding intermediate layers [15], [37], [38], [39] or by enhancing output representations [40], [41], [42]. We are excited to see that the non-local operator is being adopted in so many different research directions. Nevertheless, in this work we focus solely on Transformer architectures, and leave comparison on the various ways in which the non-local operation may be integrated into different architectures to future work.

The structure of the paper is as follows: Sec. 2 introduces the original Transformer architecture and several modifications widely adopted by video models; Sec. 3 delves into VTs in depth; Sec. 4 discusses action classification and analyses performance of various VT designs; finally, Sec. 5 discusses main trends, limitations and future work for VTs.

2 THE TRANSFORMER

We here first introduce Transformers and then illustrate the major trends seen across all Transformer-based architectures which have also been adopted for video.

2.1 Preliminaries

The Transformer [1] was first proposed as a remedy to some limitations of sequence modeling architectures. It was originally designed to deal with whole sequences at once, which allows to parallelize some operations (as opposed to RNNs, which are sequential in nature), and reduce the locality bias of traditional networks (such as CNNs).

Self-attention. SA is the core component of the Transformer. It receives the input representation $\mathbf{X} \in \mathbb{R}^{T^{(X)} \times d_m}$ and a memory $\mathbf{M} \in \mathbb{R}^{T^{(M)} \times d_m}$, where $T^{(\cdot)}$ is the sequence length and d_m is the dimensionality of each element in the sequence (namely *tokens*). In practice, $\mathbf{X} = \mathbf{M}$, hence the name self-attention. But this may be not necessarily the case, and when $\mathbf{X} \neq \mathbf{M}$, the same operation is denoted as cross-attention (CA). This type of attention is already seen in [1] when the decoder attends to the encoder representation and, in general, it provides a way to incorporate external information \mathbf{M} . In each Transformer layer, \mathbf{X} is mapped to a set of queries $\mathbf{Q} \in \mathbb{R}^{T^{(X)} \times d_k}$, while \mathbf{M} is mapped to a set of paired keys $\mathbf{K} \in \mathbb{R}^{T^{(M)} \times d_k}$ and values $\mathbf{V} \in \mathbb{R}^{T^{(M)} \times d_k}$, where $d_k = d_m/h$ and h is the number of heads (defined below).

In the Transformer, the affinity in the non-local operation is instantiated as the dot-product between \mathbf{Q} and \mathbf{K} . The resulting matrix is then used to weigh how much each value contributes to the output representation of every other

value. Intuitively, this dot-product establishes the relevance that each value has for a given query, and weighs the interactions among values accordingly. More formally:

$$\text{Att}(\mathbf{Q}, \mathbf{K}, \mathbf{V}) = \text{softmax} \left(\frac{\mathbf{Q}\mathbf{K}^T}{\sqrt{d_k}} \right) \mathbf{V}. \quad (1)$$

Transformer Layer. A complete Transformer layer (see Fig. 1a) is composed of two or more *sub-layers*, followed by a residual connection and layer normalization [43]. More formally, the output of each sub-layer, which is fed as input to the next, is defined as $\text{LayerNorm}(\mathbf{X} + \text{Sublayer}(\mathbf{X}))$. $\text{Sublayer}(\mathbf{X})$ is the function implemented by the sub-layer itself: either Multi-Head Attention (MHA) or *position-wise Feed-Forward Network* (FFN) [1] which we define below.

Similar to the multiple filters in a convolutional layer, MHA was proposed in [1], where \mathbf{X} and \mathbf{M} are mapped to h different representation sub-spaces (i.e., different sets of \mathbf{Q} , \mathbf{K} and \mathbf{V}) in order to perform different attention operations simultaneously. The output of each head is concatenated and mapped back to a common d_m -dimensional space through a linear transformation $\mathbf{W}^{(O)} \in \mathbb{R}^{(h \cdot d_k) \times d_m}$:

$$\text{MHA}(\mathbf{X}, \mathbf{M}) = \text{Concat}(\text{head}_1, \dots, \text{head}_h) \mathbf{W}^{(O)}, \quad (2)$$

where $\text{head}_i = \text{Att}(\mathbf{X}\mathbf{W}_i^{(Q)}, \mathbf{M}\mathbf{W}_i^{(K)}, \mathbf{M}\mathbf{W}_i^{(V)})$,

and $\mathbf{W}_i^{(\cdot)} \in \mathbb{R}^{d_m \times d_k}$. Note that each sub-layer will have different weights \mathbf{W} , we omit that for simplicity.

While it has been found that the non-local mixing of tokens (which happens in the SA operation) is the key for the success of many recent models (e.g., [44] and [45]), including the Transformer, it is not enough to build a successful model [46]. In practice, every Transformer layer contains at least one MHA sub-layer performing either self- or cross-attention and ends up with a final FFN sub-layer in charge of transforming the data representations. FFN is composed of two linear layers with ReLU activation function in between, i.e., $\text{FFN}(\mathbf{x}) = \text{ReLU}(\mathbf{x}\mathbf{W}_{F1})\mathbf{W}_{F2}$, where $\mathbf{x} \in \mathbb{R}^{d_m}$ is the embedding corresponding to one token, and $\mathbf{W}_{F1} \in \mathbb{R}^{d_m \times (4 \cdot d_m)}$ and $\mathbf{W}_{F2} \in \mathbb{R}^{(4 \cdot d_m) \times d_m}$ are weight matrices. In practice, an FFN is equivalent to applying two FC layers in a point-wise fashion, i.e., independently to each token. Note that each FFN layer will have different weights, but we have omitted those for ease of notation.

Masked Self-attention. The SA operation can optionally use a mask to ignore certain tokens. The idea is already introduced in [1] for the masked SA sub-layer in the decoder, such that tokens not yet predicted could not be attended. Provided that in SA $\mathbf{M} = \mathbf{X}$, the result of the dot product $\mathbf{Q}\mathbf{K}^T \in \mathbb{R}^{T^{(X)} \times T^{(X)}}$ is a square matrix. The mask is then defined as $\mathbf{M} = (m_{ij}), 1 \leq i, j \leq T^{(X)}$ and set $m_{ij} = -\infty$ iff $i < j$ and $m_{ij} = 0$ otherwise. The mask is then added to the result of normalized dot-product in Eq. (1), just before the softmax. In this way the exponential function in the softmax draws the attention values for the masked attention pairs to 0, ignoring their contribution to \mathbf{V} .

Positional Encodings (PE). The SA operation and, by extension, Transformers, are permutation-invariant. In order to incorporate structural biases in the attention computation, [1] proposes adding *absolute* positional encodings to the input sequence, \mathbf{X} , prior to SA. The encodings $\mathbf{E} \in \mathbb{R}^{T^{(X)} \times d_m}$,

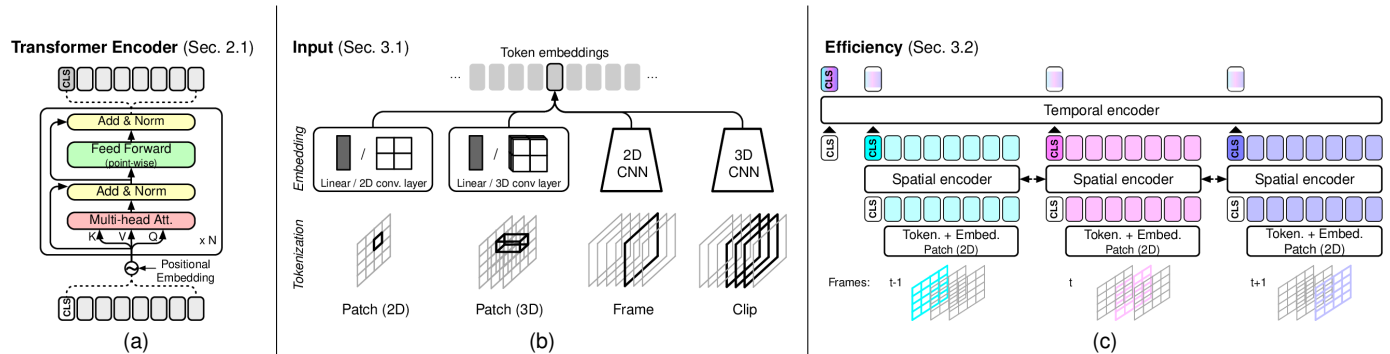


Fig. 1. General pipeline of Video Transformers (VTs) (best viewed in color). In (a) we show a vanilla Transformer Encoder [1] (outlined in Sec. 2.1); in (b) we show different tokenization and embedding strategies, which are detailed in Sec. 3.1; and, in (c) we show a common hierarchical Transformer design which decomposes spatial and temporal interactions of patches from video. These and other video designs are described in Sec. 3.2.

apart from absolute, are *fixed* as its elements are defined using a set of sinusoidal functions (also known as Fourier features, see [1] for details).

2.2 Transformer trends adopted for video

Since [1], many variations to the Transformer have become common. Although they are not particularly designed for VTs, they are often utilized and, hence, worth discussing.

Architecture. The Transformer layer we have described so far has been used to build different architectures. These can be roughly categorized into encoder-only [2], decoder-only [47] and encoder-decoder [1]. In *encoder-only* the input embedding representation is repeatedly augmented along its layers to aggregate global information in all the tokens and from all the tokens [9], [11], [48], [49], [50]. This is particularly useful for tasks that expect a fixed-sized output (e.g., video classification). *Decoder-only* rely entirely on previously decoded tokens as input, although a number of initial tokens (often referred to as *prompt*) are normally used to serve as initialization. In practice, decoder-only models in vision are mostly used to autoregressively decode captions describing visual input data. Prompting video frames will mix two very different representations in the decoder, so CNNs substitute the encoder to provide context [51], [52], [53]. Both encoder-only and decoder-only layers consist of SA and FF sub-layers interleaved with Add+Norm after each of them. In the case of decoder-only, it generally includes masking in SA. In *encoder-decoder* layers, the decoder also includes a CA sub-layer after SA, which allows it to attend to memory embeddings (sometimes referred to as context) provided by the encoder. In video, encoder-decoder architectures are exploited mostly for captioning [54], [55], [56], [57], [58], [59] and video generation [60], [61], [62]. These three configurations, however, are not the only possibility. Multiple encoder-decoder pairs can be applied in parallel [62] or sequentially [63], encoders can run in parallel [50] or hierarchically [64], [65], or encoder+decoder can be combined in a single module [58], [66].

Special tokens. Some special tokens have been proposed with different objectives. On the one hand, [CLS] is used to aggregate information from all the tokens into a single vector-form representation [11]. Although using a particular token instead of [CLS] is possible, this biases the predictions towards it [67]. Alternatively one could use avg/sum/max pooling [68], [69], [70], or weighted token

summation [71]. On the other hand, [MASK] is used to replace tokens either to predict them for the self-supervised learning of video/multi-modal representations [13], [14], [50], [72] or as a side task for training [53].

Positional embeddings: fixed or learned, and absolute or relative. Alternatively to *sinusoidal* (or *fixed*) absolute positional encodings (APE) (see Sec. 2.1), one can opt for *learned* APE, which are trained as additional network parameters [2]. Instead, *relative positional embeddings* (RPE) signal the position of one token relative to another, and can also be fixed or learned (see [73] for more details). Lately there has been a growth on works adopting RPE [12], [52], [60], [74]. We will discuss this in more detail in Sec. 3.1.3.

Activation in FFN: ReLU vs GeLU. Earlier NLP [2], [47] and image-based works [7] introduced the use of GeLU [75] (instead of ReLU) as the activation function for the hidden layer in the FF sub-layer. This trend has been followed by a number of video works [9], [49], [64], [67], [71], [76] (see Tab. 1). In particular, [71] claimed GeLU to perform the best for videos among not only ReLU but also ELU and SELU.

Pre-/post-normalization. Both [1] and [2] are examples of *post-normalization*, i.e., normalization is applied after the skip connections bypassing the MHA/FFN sub-layers. Alternatively, [77] proposed *pre-normalization*, i.e., normalization before MHA/FFN within the residual branch. In video, there are works following pre-norm (e.g., [11], [48]), but others still follow post-norm with [78] or without normalizing the input embeddings (e.g., [10], [57]) as seen in Tab. 1. Non-video works have shown pre-norm to stabilize training and reduce the need of warm-up [79].

Additional masking uses. On VTs we find the use of decoder-based masking to avoid attending at future tokens [60], [80], already attended objects [63], or not yet generated words for captioning [51], [54]. However, the literature has generalized masking in different ways, and we also find some of these in video. For instance, some works apply masking in the encoder instead, in order to focus the attention over subsets tokens [57], [59], [81]. Some other works turn unwanted tokens to 0-valued vectors instead [59] or propose using soft masks to differently weight the contribution of each token [52], [57], [82]. It is important to note that masking is not reducing the computational burden of SA, as the number of tokens is unchanged (see Sec. 3.2.1).

2.3 Transformer Limitations

Transformers have two key limitations: first, the *quadratic complexity* ($\mathcal{O}(T^2)$), which will be specially problematic for video. As we discuss in Sec. 3.2, some works try to repurpose the Transformer to better handle video data. This is generally done by reducing the sequence length when computing the attention matrix, either by restricting the number of tokens of a single attention operation, or by progressively aggregating information through contextual operations. The second limitation is the lack of *inductive biases*. While this property allows for a general-purpose architecture which produces versatile representations, it can also hinder learning unless large quantities of data are used [7] (generally through self-supervised losses [2]). We will explore how video models overcome this limitation in Sec. 3.4.

3 VIDEO TRANSFORMERS (VTs)

The high dimensionality of video data and the aforementioned limitations of Transformers demand for several adaptations in order to build successful Video Transformers. Here we perform a holistic overview of VTs: in Sec. 3.1 we explore how videos are handled prior to feeding them to the Transformer, exploring backbones for dimensionality reduction and tokenization alternatives. Then, in Sec. 3.2, we detail proposals for efficient Transformer designs, such as explicitly leveraging temporal structure in videos. Next, we analyse how is video integrated with other modalities in Sec. 3.3. Finally, we overview VT training strategies and losses, particularly focusing on self-supervised approaches in Sec. 3.4. For a comprehensive list of all VT works reviewed in this survey, we refer to Tab. 1.

3.1 Input pre-processing

Next, we review how video is processed before being input to the Transformer. This involves embeddings and tokenization (see Fig. 1b), as well as enhancing the features with positional information.

3.1.1 Embedding

In NLP-based Transformer approaches, tokenization precedes the embedding. Tokens are formed, looked-up in a table to build a numeric but discrete representation (e.g., one-hot encoding), and finally embedded into a continuous space. Differently, many vision Transformers, and especially video ones, first embed the raw data into a more compact representation that can be then used directly as a token or be further “tokenized” (i.e., divided) into more atomic units. For instance, defining as tokens the different positions of an activation map from an intermediate layer of a CNN. We refer to this as *backbone embeddings*. In contrast, *minimal embeddings* are obtained by following the classical tokenization-then-embedding approach. Inherently, minimal embeddings are guaranteed to not share information among themselves before being input to the Transformer.

Backbone embeddings. Using large backbones could alleviate the learning workload of Transformer layers not only by offering inductive biases, but also by helping to reduce the size of the input, thus avoiding to some extent the high redundancy of video data. The Transformer will

then be able to focus on enhancing higher level semantics with its wider receptive field. We can roughly categorize the backbones as spatial and spatiotemporal. Within the former, we find 2D CNN networks pre-trained on large image corpora (typically ImageNet [143], [144]) to have general filters that can extract meaningful representations of individual frames. This has been shown to work effectively, for example, in [41], [58], [86], [92], [101], [115], [119], [145], but simple 2D convolutions are unable to leverage any temporal information in this way. For this reason, other approaches [10], [37], [65], [86], [101] utilize 3D variants of ConvNets, such as I3D [87] and S3D [85], pre-trained on large video datasets such as Kinetics [146], [147] or HowTo100M [148] to produce features exploiting temporal relationships as well. Alternatively, [126] borrows from NLP and utilizes LSTMs to embed local temporal information into the input. Works using a hybrid ConvLSTM [149] are also found [62], [123]. Finally, in some instances, networks pre-trained to perform an auxiliary task (regarded as *experts*) are used to pre-process the input and provide specific information that can be leveraged by the Transformer [66], [131]. Some examples include object detection [80], action features [13], or scene, motion, OCR and facial features, among others [104].

Minimal embeddings. Inspired by the success of ViT [7], few video methods omit the use of large backbones and perform linear projections or convolutions instead, in order to embed tokens representing smaller portions of the input video [7], [9], [11], [88], [115], [130]. Empirical studies like [9], [130], show that *stand-alone Transformers* (i.e., without complex CNN backbones) are as performant as CNN counterparts, even at the expense of high computational and data resources. For very small tokens, embedding could even show little to no improvement [12]. Nonetheless, training and deploying these approaches can be computationally prohibitive, and hence, it is much less common (see Tab. 1).

3.1.2 Tokenization

As Transformers are inherently designed to model sequences, it is necessary to reshape any input data into a set of elements. We denote this process as tokenization. We distinguish between patch, frame, and clip tokenization.

Patch Tokenization. Most VTs follow ViT [7] and employ a 2D-based patch tokenization [9], [88], [114], [138], dividing the input video frames into regions of fixed size $h \times w$. For instance, 16×16 [9], [88], [138] or even multi-scale patch tokenization, ranging from 9×5 to 108×60 [114]. Others propose using 3D patches instead [11], [12], [48], [49], taking into account the time dimension in small $t \times h \times w$ regions (e.g., $4 \times 16 \times 16$ [49]). Besides, a few works propose using overlapping 2D [115] or 3D [48] patches. We also regard positions of intermediate feature maps from convolutional backbones or pooled representations of localized objects as patches. While it is difficult to determine a priori the exact receptive field of these tokens, they contain information of patches in the input. On the one hand, [82], [115], [117], [122] use intermediate representations of 2D ConvNets, whereas [86], [95] use 3D. On the other hand, a Faster R-CNN [89] can be used to extract localized object features as in [10], [13], [66].

Frame Tokenization. In this case the backbone learns initial local-based spatial features for each frame, and the Transformer focuses on modeling the temporal interactions among the resulting frame tokens. This allows longer videos to be modeled (specially compared to patch tokenization), making it more suitable for modeling longer-term dynamics. Some tasks focusing on frame-level predictions (such as video summarization [40]) may not require finer patch-level based granularity. Many VTs leverage frames as tokens (e.g., [14], [57], [59], [66], [67], [69], [93], [114]), achieving a good balance between computational cost and performance.

Clip Tokenization. Condensing the information of several frames (clip) into each individual token allows further reducing the temporal dimension of the input. This way, the Transformer can effectively consume more frames to cover longer temporal spans. This makes clip tokenization very suitable for long-term modeling tasks. Several video works explored this approach: [53] with C3D, [13] with 3D ResNet-50, [50] with S3D, [76] with R(2+1)D, or [64] with SlowFast, to name a few. This tokenization could also be suitable for retrieval tasks, where a high-level representation of the video is required [13], [104]. Similarly, this is used for ease of alignment between modalities (e.g., [65], [71] pair small clips with textual captions). However, depending on the size of the clips, fine-grained information may be lost or mixed (e.g., the location of objects), preventing the Transformer from disentangling it later.

3.1.3 Positional Embeddings

Given that SA is an operation on sets, signaling positional information of structured data has proven effective for Transformers. VTs have used fixed APE [10], [48], [123], learned APE [13], [64], [130], fixed RPE [58], [61], or learned RPE [12], [60], [128]. Absolute variants are commonly summed to the input, but can also be concatenated [122], [124], [130]. This consideration is not required for relative ones, which are instead incorporated during MHA [73].

Absolute embeddings are generally 1D. This naturally fits frame or clip tokenization to indicate position in the temporal dimension. However, when dealing with patches, fixed 1D in raster order may seem counter-intuitive, as the last patch i from row j , will be regarded as closer to the first patch at row $j + 1$, than to patch i at row $j - 1$. For this reason, 2D APE [80], [95] accounting for space wh and time t dimensions and 3D APE [88], [123], [130] for width w , height h , and t have also been proposed, disregarding [7] who found learned 1D APE to suffice – at least for images.

The idea behind RPE is that the positional information added when computing attention between token i and j depends on their relative position. In other words, the RPE added when computing attention between token at position i and $j = i + k$ will be the same regardless of the value for i (i.e., $-k$). Recent advances on RPE in NLP [150], [151] with respect to the earliest works [74], [152], have motivated its use also for video. While most of the other works are based on [74] (e.g., [12], [52], [60]), [128] follows the approach of [152]. Interestingly, [58] encodes relative positional information as in Transformer-XL [150], which is a generalization of [152] that adds extra bias terms. One clear advantage of RPE is the possibility to test on sequences of different length without negatively impacting performance, although some

video works have explored the interpolation of APE [48], [49] for longer sequences at inference time.

3.1.4 Discussion on input pre-processing

Most VTs employ large CNN backbones to reduce input dimensionality (aiding with data redundancy) and to exploit their ability to produce strong representations (thanks to local inductive biases). This significantly alleviates complexity and simplifies training when employing Transformers for video tasks. The success of these methods is clearly visible by the amount of works which utilize backbone embeddings as opposed to minimal embeddings (see Tab. 1). Regarding tokenization, it has an impact on two main factors: (1) it will affect the level at which information is modeled by the VT (longer span temporal modelling through frame- or clip-based tokenization, and more fine-grained spatiotemporal modeling when employing patches); (2) it will impact the input sequence length, and consequently the memory complexity of the model. For these reasons, most works use a patch-based approach accompanied by some efficient design, or frame based tokenization, as it presents a better performance/complexity trade-off. Finally, most of current research still employs the fixed APE (see Tab. 1) proposed in [1], as they require less parameters than the learned counterpart. However, the latter could be learning relevant positional relations that Fourier-like approaches are unable to capture (similarly to how learned convolutional filters replaced manually designed ones from traditional image processing). Furthermore, most works define a fixed input length, either by cropping or sub-sampling the original video, and very few have tested interpolation at test time [48], [49]. In this sense, RPEs seem to be a promising research direction, as they generalize to unseen lengths. Nevertheless, how the choice of PEs impact performance, and whether learned PEs have any real advantage over fixed ones has yet to be thoroughly investigated.

3.2 Efficient designs

Given the high dimensionality of video it can be challenging to represent long sequences without incurring in information loss (through dimensionality reduction) or stumbling upon the quadratic attention matrix problem when modeling them. For this reason, while the use of large backbones focuses on reducing dimensionality, the key architectural changes proposed for VTs focus on reducing the size of the attention matrix. Two main trends are observed: (1) *restricted* approaches, which reduce the number of tokens attended in a single SA operation, but maintaining the number of tokens throughout the network; and (2) *aggregation* approaches, which focus on progressively condensing information, mostly through hierarchical approaches that gradually reduce the number of tokens. In an orthogonal direction, we also discuss approaches to improve parameter efficacy by *weight sharing* or low-rank approximations of the attention matrix. A complete overview of our proposed taxonomy for efficient video designs can be seen in Fig. 2.

3.2.1 Restricted approaches

Restricted approaches can be roughly categorized in: *local*, which limit attention to specific token neighborhoods; *axial*, which restrain attention within a specific dimension (i.e.,

height, width or time); and *sparse*, that only attend a subset of tokens, which can be arbitrarily far away. When leveraging one of these approaches, the receptive field of the SA operation is notably reduced. In order to compensate for this, it is common to approximate the receptive field of full attention by stacking several restricted attention operations sequentially. This is conceptually similar to convolutional layers: by stacking several local filters, the receptive field of deeper layers is effectively the whole input.

Local approaches are defined as the restriction by limiting attention to specific neighborhoods. Local restriction approaches reduce computational complexity from $\mathcal{O}(T^2)$ to $\mathcal{O}(T \cdot N)$, where N is the size of the neighborhood. One set of works [9], [99], [99], [119], [131], define the neighborhoods by sampling nearby tokens given a query, similar to the sliding window approach in the NLP Longformer [153]. Importantly, in [99], the [CLS] token does perform all-to-all attention. Other works [12], [60] have proposed limiting SA to small fixed windows instead. To allow for information flow between different regions, [60], [119] employ different neighborhood sizes in each head, while [9] alternates between local and sparsely global attention. Instead, [12] proposes shifting the windows on every layer.

Axial approaches. Axial approaches define the restriction to attention by specific axes. These can only be applied in patch-based tokenization models. While full axial attention decomposition (i.e., into h , w , and t axes) has been tested for VTs [9], the most commonly used is spatiotemporal decomposition: spatial attention computes inter-frame interactions and temporal attention is in charge of learning intra-frame relationships. Spatiotemporal decomposition reduces computational complexity from $\mathcal{O}((t \cdot w \cdot h)^2)$ to $\mathcal{O}((w \cdot h)^2 + t^2)$. These approaches are implemented in one of two fashions: (1) employing two consecutive MHA sub-layers, one spatial and one temporal [9], [11], effectively alternating between both types of interactions on each layer; and (2) using first a full spatial attention module, followed by a temporal one to attend to other frames [80], [90], [131]. However, in [11] dividing the heads within one MHA module into spatial and temporal heads is also explored. Finally, in [117] T temporal and HW spatial features are produced by separate pooling operations, which are then concatenated.

Sparse approaches. Opposed to local and axial approaches, sparse restrictions do not limit the scope of attended tokens. The most traditional approach for sparse attention uses strided global attention, where at most every other token is accessed by a given query. In [9] it is alternated with local attention operations. On a different note, VATT [49] proposes *DropToken* to reduce input resolution by dropping a fixed ratio (in practice, 50%) of tokens, which also serves as regularization. VATT demonstrates improved performance by dropping tokens compared to reducing resolution through CNN backbones. In a similar fashion, [134] uses Farthest Point Sampling [154] to select a restricted subset of tokens from a large sequence of past observations (memory). This is processed by a two-step encoder: the first step augments the queries from the restricted subset by cross-attending to the whole memory; and in the second step, the complete memory is embedded into queries that attend over keys and values from the restricted subset.

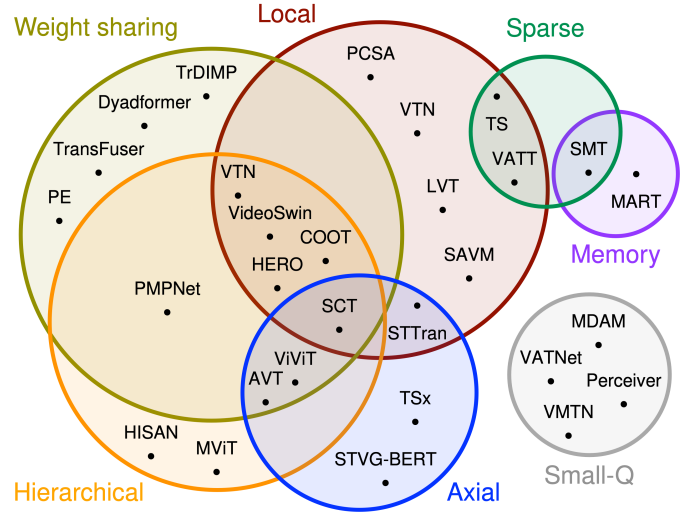


Fig. 2. Venn diagram displaying our proposed taxonomy of efficient VT designs (best viewed in color). TS (TimeFormer) and TSx [9], STVG-BERT [117], SCT [90], AVT [80], ViViT [11], SAVM [60], LVT [61], HERO [14], VideoSwin [12], VATT [49], MVIT [48], COOT [71], SMT [134], Perceiver [130], STTran [131], VATNet [10], MART [58], HISAN [81], Dyadformer [142], PE [64], VTN [99], VMTN [129], PCSA [119], MDAM [55], VATT [49], TrDIMP [82], PMPNet [42], and Transfuser [132]. We describe Local, Axial and Sparse approaches in Sec. 3.2.1, Hierarchical and Small-Q(eries) in Sec. 3.2.2 and Weight Sharing in Sec. 3.2.3.

3.2.2 Aggregation approaches

It is customary that Transformers are isomorphic across layers (i.e., maintain feature dimensionality). This allows for easy tracking of tokens across the layers and the use of residual connections without additional parameters. Some VTs, such as [12], [48] are found to progressively aggregate information while expanding the number of channels. This spatial downsampling, however, requires more weights for the latter layers, as the matrices grow with the number of channels. Due to Transformers’ ability to encode highly contextual representations, they themselves can be employed to aggregate information (generally through the [CLS] token). While this is not necessarily efficient on its own (for instance, when used as final representation for computing a classification score [7], [11], [13], [50], [141] or measuring similarity for retrieval [69], [104], [108]), this idea can be used to build efficient models. Such is the case of *hierarchical* approaches and the use of a *small queries*, which iteratively condensate information in a small set of tokens.

Hierarchy. Several hierarchical video architectures have been proposed. On each stage, different subsets of the input tokens are independently processed through separate Transformer modules, for intra-group relationships. This is equivalent to weight sharing or batched-like processing. Then, information from each subset is aggregated and fed into the next stage, which models inter-group relationships. Hierarchical approaches are a way to infuse inductive biases in the design, as they force different layers to focus on learning different levels of data interactions, thus making a more effective use of parameters. Furthermore, as information is aggregated progressively, deeper layers end up having to deal with less tokens when compared to an equivalent Transformer without hierarchy, hence achieving an improved computational efficiency.

One subset of works learns spatial patch-wise interac-

tions in the first stage (generally through a ViT like [7] architecture), and temporal frame-wise interactions in a second stage [11], [80], [99] (see Fig. 1c). The work of [90] goes further and uses a first layer to learn interactions among small patches within a limited frame window. Then, they perform efficient global patch attention thanks to using *Locality-Sensitive Hashing* [155] (inspired from the efficient NLP Reformer [156]). In [42], temporal fusion is handled differently by using a combination of GRU and Transformer layers. Spatiotemporal hierarchy approaches allow for independent pre-training of the spatial layers on large image datasets, which helps to boost performance.

Another subset of works focuses on local interactions in the first stage and longer term interactions later. For instance, [71] models short frame neighborhoods independently first, which are later aggregated into clips. A second stage processes interactions between those. Interestingly, instead of using the [CLS] token, the authors find that using a few linear layers to generate an aggregation weighting matrix works better in the context of video retrieval. On a different note, [14] proposes learning short-term cross-modal interactions of frames and subtitles. Then, only the subtitle-enhanced video tokens are fed to a temporal Transformer, in charge of learning long-range dependencies. Finally, [81] uses object features as queries to aggregate contextual information, for later fusion of appearance and flow features.

Small Queries. Another way to reduce computational complexity of the attention matrix consists in reducing the number of queries. The main idea is to use a set of queries \mathbf{Q} such that $T^{(Q)} \ll T$. That way, memory requirements of the model are reduced from $\mathcal{O}(T^2)$ to $\mathcal{O}(T \cdot T^{(Q)})$. In this way, the actual feature representation is smaller ($T^{(Q)}$) and iteratively refined by successive accesses to the complete input representation. Firstly proposed in [10], a Region Proposal Network (RPN) is used to extract a small set of boxes from the input clip. The features from those regions are used as queries while keys and values are from the whole embedding volume. The work of [129] extends on this idea through a two stream network. However, instead of using an RPN to form the queries, they perform feature aggregation by linearly transforming the feature map into a matrix that weights how much should each token contribute to the final representation. Similarly, [55] uses a small query set derived from a language question, while keys and values are the complete visual features. The use of a small \mathbf{Q} is also seen in [71], which leverages a global stream to generate a whole sequence aggregation token. This is used as query in a last global attention stage to attend to clip tokens for a final compressed video representation. It is also interesting to highlight the case of [58], which maintains a fixed-size memory that progressively aggregates information from past iterations by combining SA and a gating mechanism. Finally, in [130] a generalization of this idea is explored: instead of using queries from a sub-sampled or aggregated version of the input data, a small set of latent (learned) query vectors are used to iteratively cross-attend the input, while their representation is further enhanced through SA layers between each of these accesses.

3.2.3 Weight sharing

Weight sharing reduces the number of parameters of an otherwise highly parametric architecture. It has been applied in many video-based works. Weights can be shared across some or all layers within a module [142], across layers in different modules [64] or directly sharing entire modules [130]. Another example is [82], which shares the weights across SA sub-layers in the encoder and decoder. Their premise is that transforming input embeddings of the two modules into the same feature space, later facilitates the task of the CA sub-layer in the decoder. As mentioned in Sec. 3.2.2, weight sharing is equivalent to batched processing or applying the same module to different clips in a video [71], spatiotemporal scales [62], and modalities [49]. In fact, most hierarchical designs share weights for the modules that process independent neighborhoods in the first stage [11], [12], [14], [80], [90], [99].

The work of [64] provided the most comprehensive analysis on weight sharing among video works. They obtained competitive results when naively sharing weights across layers in the same module or across all the layers in the architecture, even when multiple modalities are used. They even shown how factorizing the weights achieved not only better performance than the rest of approaches (not sharing included), but also the lowest number of parameters. To do so, they factorize the linear transformations (i.e., \mathbf{W}) in Transformer layers using low-rank approximation: $\mathbf{W} \mathbf{x} = \mathbf{U} \mathbf{\Sigma} \mathbf{S}^T \mathbf{x}$, where \mathbf{U} and \mathbf{S} are projections and $\mathbf{\Sigma}$ is a rotation after applying several linear algebra tricks. Whereas $\mathbf{\Sigma}$ and \mathbf{S} are private for every layer, \mathbf{U} are the shared weights.

The only VT work to report negative influence of weight sharing is [132]. However, differently from [64], Transformer layers are interleaved with convolutions that keep reducing the spatial size and increasing the number of channels, enormously changing the nature of the features modeled at each stage.

3.2.4 Discussion on efficient designs

Most adaptations for efficiency focus on reducing the complexity of the attention operation. Composing several restricted attentions with their span limited to subsets of tokens still allows for comparable results to all-to-all attention, making these suitable for VTs. Similarly, aggregation seems to be a promising research direction, given its capabilities for video compression based on context, as opposed to pooling or other aggregation techniques. Another possibility to increase efficiency is to reduce the number of parameters via weight sharing, and hence alleviating memory consumption without sacrificing performance. Nevertheless, while we find many interesting approaches to address the complexity of video data with Transformers, the main trend still is to use off-the-shelf Transformer architectures with either strong backbone dimensionality reduction or heavy computational budgets. There are lots of room for improvement, both in terms of efficiency (see [19], [20]) and better exploiting inherent features of video data.

3.3 Multi-modality

The human experience of the world is inherently multi-modal. Studies in both Psychology [157] and Computer Vision [158], [159] have consistently found that multi-modality

provides useful cues for learning without the need for supervision [160]. This, tied with the versatility of Transformers for handling any type of data, leads into many VTs to be deployed in multi-modal settings.

One very generalized multi-modal approach is to leverage *multi-modal fusion* (Sec. 3.3.1) strategies to combine the embeddings of different modalities into a joint multi-modal representation. When done properly, it allows to exploit potentially present complementary cues across modalities and reinforce cross-modal information. However, Transformers are not task-agnostic, but also consider architecture-related modifications for particular pretext and/or downstream tasks. In particular, for *multi-modal translation* (Sec. 3.3.2), the non-video embeddings are input to the decoder and autoregressively produce the output by incorporating contextual video (or multi-modal) information provided by the encoder. In the following section we cover multi-modal fusion and translation. Then, in Sec. 3.4.2, we discuss *multi-modal alignment* that, differently from the previous two, does not require architectural changes, but is performed during training via contrastive learning. Furthermore, in the supplementary material we briefly detail how the different modalities are embedded when used in the context of VTs (Sec. S1.1).

3.3.1 Multi-modal fusion

Video can be fused with many modalities, but most often with audio [54], [130], text [13], [50], [58], and optical flow derived from the video itself [76], [86], [95]. Some challenges when fusing modalities is difference in size, sampling rate, or the redundancy of their contained semantics. Text is much lower dimensional than video, but at the same time it provides useful high-level semantics that could help pinpoint salient parts of the video or establish priors about its relationships. In contrast, audio is sampled at much higher frequencies than text and hence SA among video and raw audio frames is impractical without embedding audio first into a more compact representation. Commonly, log-mel spectrograms are used to represent relatively long-term temporal audio chunks into a 2D image-like representation that can be input to an off-the-shelf 2D-CNN [161].

To fuse modalities, Transformer-based strategies typically rely on the concatenation of input sequences from all input modalities or, alternatively, on some form of cross-attention (see Fig. 3). Within the first alternative, we distinguish *encoder fusion* and *hierarchical encoder fusion*. Among cross-attention based strategies, we find *cross-attention fusion*, which is one-sided attention of one stream over the other, and *co-attention fusion* where two streams attend to each other simultaneously. The latter two are typically implemented as encoder-like Transformer layers but modified to include CA sublayers, i.e., decoder-like layers but without the masking (and occasionally dropping the initial SA sublayer). Moreover, we not only discuss “how” but also “where” the fusion takes place in the architecture, i.e., early, middle, or late stages.

Encoder fusion (EF). Before being input to the encoder, the token embeddings of different modalities are concatenated either sequence-wise [14], [50], [70], [101], [104] (see Fig. 3a) or channel-wise [134]. One can think of the former as how BERT [2] deals with pairs of language sentences. In order

to identify which tokens belong to each modality, [50] uses separator tokens in a similar fashion as [SEP] in BERT, originally used to indicate that a new sentence is starting, adapted here to indicate that the following tokens are from a different modality. Most VTs, however, signal the modality of a given token by summing (or concatenating) learned *modality embeddings* [13], [64], [69], [70], [104], similar to the way in which PEs are added. Encoder fusion considerably increases the computation cost of the SA operation up to $\mathcal{O}((T_1 + \dots + T_M)^2)$, where M is the number of modalities and T_m the number of tokens in the m -th modality (for further details see Sec. S1.2).

Hierarchical encoder fusion (HEF). Encoder fusion can also be done hierarchically by augmenting modality-specific token embeddings on individual encoders first, concatenating their outputs, and sending those to a multi-modal encoder [64], [65], [66] (see Fig. 3b). This kind of fusion allows intra-modal information to be handled before modeling the inter-modal patterns, which can be beneficial when dealing with modalities that are not highly correlated or precisely aligned at the input level. The point at which to do so has to be determined experimentally. Also, computational cost is reduced with respect to the previous encoder fusion by a constant factor, depending on the number of layers in both the uni-modal and the multi-modal encoders. Although utilizing multiple encoders increases the amount of parameters, this can be alleviated through weight sharing [64] (see Sec. 3.2.3).

Despite being more rigid, encoder fusion allows for an unbounded number of modalities. Cross-attention, even when limited to two modalities only, allows for more flexible modality fusion. We distinguish between cross-attention (one-sided) and co-attention (two-sided), the first being from one modality over another and the second being mutually conducted in parallel.

Cross-attention fusion (CAF). When fusing modalities through CA, one modality will query information from an auxiliary modality that will provide context (see Fig. 3c). The simplicity of this idea together with the flexibility it provides, causes many works to use it very differently. In [55], [56] separate encoder-decoders for each modality are proposed, each cross-attending to text embeddings, before the outputs of the different encoders are combined. The work of [130] proposes only one stream that keeps augmenting a small set of latent embeddings by repeatedly cross-attending to the same very long multi-modal input sequence of minimal embeddings. For this case, CA layers are interleaved with SA layers that refine the cross-attended information. In [13], a three-stream Transformer is proposed where the central one cross-attends to the other two, and these will then attend to the embeddings generated by their respective opposite previous cross-attentions. The work of [136] also uses three streams, one per modality. The fusion, however, is achieved within a master stream which substitutes its SA by asymmetric cross attention over the other two at the same time (concatenating both sets of keys and values). CAF only involves two modalities at once, but has a reduced cost compared to encoder fusion, i.e., $\mathcal{O}(T_1 \cdot T_2)$. Notably, asymmetric attention allows the master stream to discard information from a specific modality when it is not relevant.

Co-attention fusion (CoAF). Differently from cross-

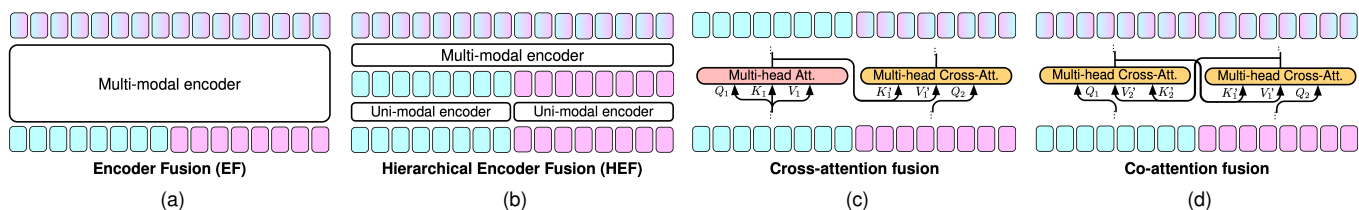


Fig. 3. Four main trends to arrange encoder modules when performing multi-modal fusion (best viewed in color). See Sec. 3.3.1 for the details.

attention fusion, the two modalities in co-attention are augmented in parallel by attending to each other’s embeddings. The CA sub-layer in each of the streams computes the queries from its own embeddings, whereas keys and values come from the other stream (see Fig. 3d). It was originally proposed for images and language in ViLBERT [162] and followed by a few video works [54], [117], [142]. In [117], [142], SA is entirely replaced by CA, but it can also be kept [54]. Indeed, [53] has their modalities co-attending to each other and self-attending to themselves, claiming this keeps intra-modal and inter-modal dynamics separate, up to some degree. In contrast to encoder fusion, the computational cost is reduced to $\mathcal{O}((T_1 \cdot T_2)^2)$.

All of these fusion strategies allow for different early and middle fusion strategies. However, another alternative is to simply late fuse modalities. In order to do that, the different modalities are run through parallel encoders and, then, their outputs are combined. These outputs could be class score distributions [95], as typically done for Two-stream ConvNets [163] in classification problems. Although suboptimal for Transformers, this strategy might still be beneficial when training data is scarce. Alternatively, late fusion could also be regarded as combining the augmented aggregation token (or pooling over all output token embeddings) by concatenation [55], [56], [76] (or summation [132]) and then using this for classification. In either case, the modalities do not share information explicitly.

3.3.2 Multi-modal translation

In the context of video literature, translation can be considered a multi-modal task: given video (and possibly additional modalities) it is translated into a set of non-video outputs. The vast majority of translation VTs are dedicated to generating language captions describing video content [14], [51], [54], [57], [58], [59]. Beyond captioning, multi-modal translation has been applied to sign-language translation [78], [136], visual-language dialogue systems [101], spatiotemporal localization [52], visual reasoning [63], or robot navigation [134], just to name a few. Most commonly exploited input modalities for the translation task along with video are text [58], [101], audio [54], [101], and optical flow [52], but others are also used (e.g., human pose [136] or depth [134]). Multi-modal translation generally uses encoder-decoder or decoder-only schemes. When multi-modal input is provided, multi-modal fusion can be adopted before the translation, following what we discuss in Sec. 3.3.1. Yet some works completely skip the prior fusion [51], [52], [101] or opt for a hybrid module that fuses and decodes at the same time [58]. Except for the latter approach, the decoder roughly maintains its canonical form. The SA layer before the CA can be removed to slim

the models [101] or substituted by a moving average [59]. The decoder layers can also cross-attend to the encoder layers of their respective depth [54], [57] or to the output embeddings of different modalities separately and average the resulting attention outputs [136]. Alternatively, the decoder can rely entirely on itself using prompt-based input, thus not relying on neither an encoder nor a backbone, as done by [101] (following GPT-2 [164]), or on external long-term memory modules [58]. Specifically, [58] proposes an hybrid encoder/decoder architecture that augments input modalities while cross-attending to a memory to decode the next sentence of a paragraph.

3.3.3 Discussion on multi-modal approaches

We have outlined two relevant multi-modal approaches that imply changes in the architecture of VTs, i.e., multi-modal fusion and translation. EF and HEF are concatenation-based fusions at, respectively, early and middle stages. HEF is computationally more expensive, but does not require experimentally validating the fusion point. CAF and CoAF are cross-attention based and inherently restricted to two modalities, although cumbersome approaches leverage this kind of fusion for more than two streams [13]. They are more efficient than both EF and HEF, yet they both have the problem of determining the best point to fuse. Still, middle fusion could help when input modalities are not perfectly synchronized or differing in nature. With regards to works exploring multi-modal translation, they find different ways to translate multiple input modalities to the output one. Multi-modal fusion can precede translation, but if that is not the case then the input modalities should be explicitly incorporated at the decoder-level.

3.4 Training a Transformer

The most common practice for training Transformers is to pre-train them on large-scale datasets [165] (either in a fully-supervised [7] or self-supervised [2] fashion) before they are transferred for a downstream task on a smaller dataset. For this, the model is either fine-tuned or linearly probed (training only one linear layer or small network on top while keeping the weights of the Transformer frozen). While several works have found data augmentation, regularization and careful tuning of hyperparameters to play a strong role in successfully training visual Transformers [166], [167] (sometimes even reducing the need for data [168]), these are not very common in video.

Vision Transformers are rarely used in a stand-alone fashion [21]. CNN backbones provide Transformers with inductive biases, as well as reduced input size, allowing Transformer layers to focus on learning higher level long-range relationships. Empirical studies on image Transformers have consistently found improvements when training

Transformers and CNN backbones end-to-end [6], [167]. Next we explore how VTs are trained considering all these variables, i.e., use of backbones, large datasets and pre-training strategy (either fully- or self-supervised).

3.4.1 Training regime

Pre-trained backbones. Backbones are theorized to aid Transformers overcome their lack of inductive biases. However, fitting both into GPU memory for training is not always an option, which is further problematic when using multiple experts, e.g., [104]. Handling several stages of training requires more time and compute power. Furthermore, properly training big models while avoiding overfitting requires strong regularization [169] and lots of data [170]. As a side note, data augmentation is computationally heavy for video [97], a modality for which its high dimensionality already poses a memory and computational burden as it is. All these result in most VTs leveraging pre-trained CNN backbones, which are then frozen and used for feature extraction. Afterwards, Transformer layers are trained for a downstream task on those features. With this approach, many works [52], [67], [78], [81], [86], [95], [101], [136], [141], [171] are still able to train the Transformer on small datasets (<10k training samples). However, it is definitely common to use medium to large datasets, as in [53], [54], [56], [57], [58], [59], [66], [93], [172]. Furthermore, it is often cheaper and more efficient to employ SOTA models, which have been carefully tuned to perform well on some supervised tasks, than training from scratch. Also, this further boosts cost-effectiveness, as it allows to pre-extract features beforehand. A subset of works do pre-train Transformer layers on some large-scale datasets for the same task as the downstream (generally smaller) dataset [40], [91], [92], [128]. For instance, in [69], authors leveraged pre-training on HowTo100M [148], which showed improved results for all 4 downstream datasets on the tasks of video-text and text-video retrieval.

End-to-End training with minimal embeddings. To ease memory limitations while allowing for end-to-end training of the Transformer, it is common to use minimal embeddings. Some train in a supervised fashion [9], [11], [48], [60], [90], [130], directly for a downstream task on large datasets, such as HowTo100M [148], Kinetics-700 [147], or even ImageNet21K [144]. Others follow a similar fashion but utilizing small datasets aided by some data augmentation [62], [88], [173]. There are also works leveraging self-supervised losses [49], [51], [80], [114], [115] on medium to large datasets. Using just a few embedding layers allows to fit the whole model into memory, easing end-to-end training. Thanks to CNN inductive biases, a few layers may be enough to learning necessary local patterns such that useful representations are fed into the Transformer.

End-to-End with backbone. Other works have leveraged full CNN backbone architectures and still manage to train end-to-end, either with a pre-trained backbone [55], [112], [117], or training it from scratch with the Transformer [82], [97], [123], [137]. Some were able to do so thanks to using only a few (from 1 to 4) Transformer layers [42], [76], [138], showing that adding a few Transformer layers right after a large backbone may be enough to boost performance. Some other’s success is attributable to leveraging efficient designs,

such as local SA [119] or weight sharing [64] – as seen in Sec. 3.2. Finally, [10], [174] report having substantial computational resources available, which allowed them to fit in memory both, a large backbone and a big Transformer. For some designs it is more natural to train end-to-end as they embed Transformer layers within the backbone, either to enhance local convolutional features across multiple ResNet streams [132], or to enhance feature representations between a CNN encoder and decoder [114], [115].

Pre-trained Transformers. A set of works have also leveraged pre-trained Transformers. It is generally the case that the models are based on image Transformers and extended to the temporal dimension. For instance, [9], [11], [80] first use a spatial Transformer (pre-trained ViT [7] on ImageNet-21K [144]) to model interactions between 2D patches in the frames, and then train the temporal Transformer on top from scratch. In a similar fashion, [12] used pre-trained weights from the image Swin Transformer [175], by inflating the linear embedding layer and the relative position biases. ST-ViLBERT [117] is initialized with ViLBERT [162] pre-trained on CC [176]. Both [63], [174] initialize their model from a pre-trained image DETR [8]. Finally, and interestingly, [50] used a pre-trained BERT [2] model as starting point for their model. They simply extended the codebook with pre-trained centroids of quantized visual tokens.

3.4.2 Self-supervised tasks

Harvesting large supervised datasets is often problematic, given the cost of manual annotations. It is for this reason that self-supervised tasks have seen widespread adoption for training Transformer models. In particular, for VTs, we see two main trends: (1) *BERT-like* and (2) *Contrastive* losses. **BERT-like losses.** BERT [2] first proposed two self-supervised losses which have been widely adapted to video. *Masked Token Prediction* (MTP) randomly masks some input tokens with a special [MASK] token. Then, the masked tokens’ output representation is trained to predict the input for that token. This forces the Transformer to learn contextualized representations of the input. *Next Sentence Prediction* (NSP) feeds the model with two sentences (divided by the [SEP] token), which are either consecutive or randomly paired. The network is trained to classify (from the augmented [CLS] token) whether they are actually consecutive or not. This helps the network to learn intra-sentence correlations and to build longer term coherent representations. Both of these losses have been adapted for video. On the one hand, MTP is used to predict masked video tokens, generally accompanied by MTP for other modalities, leveraging multi-modal contexts to help learn inter- and intra-modal representations. On the other hand, NSP is used to match correct pairs from different modalities.

Masked Token Prediction. Different from text, visual tokens are highly dimensional and continuous. For this reason video MTP can not be directly posed as a classification task, as explicitly reconstructing the whole input token may be too costly. Some works [14], [72], [177] have tried regressing masked token embeddings through an L2 or MSE loss function. However, in [14], they find this implementation to not contribute much when compared to other alternatives. Other approaches involve discretizing video tokens using quantization [50] or classifying the contents

present in them [13]. Also, in [53] authors propose an asymmetrical use of MTP where only textual tokens are masked, but visual context is used to reconstruct them. The most common approach, however, is found in other works that propose adapting a variant of the *Noise Contrastive Estimation* (NCE) [178], which we detail when discussing contrastive losses.

Cross-modal Matching. It is an extension to NSP, commonly used for learning alignment between modalities. The representation from [CLS] tokens is used to decide whether paired samples from two modalities match. To form false pairs, one modality is randomly sampled from the dataset (e.g., a subtitle from other video). It is posed as a classification task, generally through binary cross-entropy [13], [50], [64]. The work of [64] builds up on this idea and aligns both at the output of the individual streams, as well as from per-modality [CLS] embeddings output by the cross-modal encoder. Also, they align randomly sampled embeddings other than [CLS]. On a different note, [14] used a cross-entropy loss to predict the probability of every position of a given video to be the start and end index positions of an input query subtitle.

Contrastive losses. Most VTs using self-supervised approaches tend to use a contrastive loss in one of two forms: the softmax version of NCE, denoted as *InfoNCE* [179], [180], or *Bi-directional Max-Margin* (BMM) loss. Contrastive approaches define one anchor \mathbf{x} , a positive sample \mathbf{y}^+ (correctly paired with the anchor) and a set of G negative samples to contrast against $\{\mathbf{y}_g^-\}$, where $1 \leq g \leq G$. They force representations for the positive pair to be similar, while it drives apart representations for the negative (dissimilar) pairs. In multi-modal settings, however, it is more common to use two anchors (one from each modality), which form the positive pair, and two negative sets. While BMM explicitly includes this in its formulation, a subset of works [70], [97] use two InfoNCE losses instead [49]. Exceptions to this are [14], [71], which use a combined hinge loss, similar to BMM but with only one negative element for each modality. **InfoNCE** is generally used for self-supervised video representation learning. Minimising InfoNCE can be seen as maximising a lower bound on the mutual information between \mathbf{x} and \mathbf{y}^+ . It does so by means of a similarity function $sim(\cdot)$, which measures the affinity between two elements. This function assigns a high score to positively correlated pairs $(\mathbf{x}, \mathbf{y}^+)$ and a low score to negatively correlated ones $(\mathbf{x}, \mathbf{y}^-)$. In VT training, $sim(\cdot)$ is generally instantiated with either the (embedded) dot-product [49], [64], [65] or cosine distance [70], [91], [97]. As a side note, the work of [68] proposes using the Circle loss [181] (performing better than InfoNCE in a video-to-video retrieval setting), which uses an adaptive penalty strength to separately optimise the similarity of positive and negative pairs, and leverages intra- and inter-class margins, similar to BMM.

InfoNCE is utilized to align feature representations of pairs of elements in three different fashions: (1) as we have already mentioned, it is used to replace log-likelihood in MTP [14], [64], [65], [91]; (2) for representation learning, it is used to drive together differently augmented versions of the same input [91], [97]; and (3) it is used for video retrieval, either in multi-modal alignment methods [49], [70] or in video-video retrieval, to learn similar representations

for similar videos [68].

InfoNCE for MTP. Instead of reconstructing the original token based on context, these approaches train the model to correctly identify it compared to a set of negative distractors. In this setting the output representation of the masked token is set to be the anchor. The positive pair is either an embedded representation of the masked token from the backbone network [14], [64] or from an external encoder [65]. The negative set is formed by other embedded tokens different from the anchor. This formulation forces the Transformer to use contextual information such that the representation of the masked token matches that of the augmented output token more than it does the other tokens.

InfoNCE for representation learning. In this case, positive pairs are differently augmented versions of the same sample. The model is trained to match output representations coming from the same input, learning invariance to the augmentations. In particular, [91] aligns augmented clip representations, through time-shifts and croppings, while also using InfoNCE for the MTP task. In [97] multiple combinations of positive pairs are used by leveraging more than two augmentations.

InfoNCE for multi-modal alignment. Here the loss forces correctly paired samples from different modalities to convey the same information. InfoNCE is the only alignment cue for those models that leverage separate streams for each modality [70], [97], generally in the context of retrieval tasks. For instance, [51] used it to drive representations from separate video and audio CNN backbones while distilling from a captioning Transformer. In [49] authors used it in a hierarchical fashion, forcing audio and video representations closer first, and then aligning the previous (audiovisual) aligned representation with the textual one. The work of [97] aligns the representations of audio and different spatiotemporal video crops. Thanks to these cropping augmentations, their model successfully learns to attend to the spatial sources of audio within the video, as seen in their attention visualizations. In the context of multi-modal fusion, [64] separately uses InfoNCE on video and audio modalities, [14] uses it to align subtitle-enhanced visual representations, and [65] for solving both video only and multi-modal MTP.

Negative Sampling. Contrastive literature has found that the size of the negative set can influence performance [182]. Given that InfoNCE is used to learn similar representations for token embeddings [14], [64], [65] or global embeddings of the sequences [49], [68], [70], [97], negative samples are mined from other tokens in the current sequence or from other sequences in the batch, to save memory. However, larger batches are not always an option due to computational limitations. For this reason, [64] proposes to focus on quality instead of quantity. They emphasize how choosing negative samples that are either too similar or too different from the anchor may hurt performance. Learning to separate somewhat similar samples may be helping the model learn small nuances which can be crucial downstream.

On a different note, [70] proposes using a large memory to sample negatives from, filled with the most recently processed batches. They leverage a Siamese network in a Momentum Contrast (MoCo) [183] fashion. In this setting, the main network is trained through backpropagation, while

its twin is a moving average. By exploiting output features from the twin network, they show improved retrieval results when compared to using features stored directly from the main network. Similarly, [68] uses a memory bank which is built by compounding batches in multiple parallel GPUs. While each batch is processed independently, negatives are sampled from all of them, achieving an effective increase the size of the negative pool.

Bi-directional max margin. Similar to using InfoNCE for modality alignment, this loss is commonly used for video retrieval [69], [104], [108]. It enforces similarity for true pairs to be higher than that of negative pairs, by at least a given margin. Importantly, and different from InfoNCE, it employs two anchors, one from each modality, which form the positive pair. Each of them is forced to be represented differently from respective negative sample sets of from the other modality.

Hierarchical alignment. While the most common approach is to contrast final output representations, other works leverage hierarchical contrastive losses. On the one hand, [71] uses a combined hinge loss after the output of the frame processing Transformer and at the output of the clip level Transformer. On the other hand, in [70] the InfoNCE loss is used at the output of the first and last layer, to force representations together since the low level features.

Other self-supervised losses. Aside from Contrastive losses, some works have also leveraged other self-supervised losses for video tasks. In [14], among other multi-modal tasks, frame shuffling is used to make the Transformer learn time consistency. Just before adding positional information, frames are randomly reordered and the task is posed as classification of each token in its correct position in the original sequence. In [80], the causally masked model is trained simultaneously to regress the next token representation as well as to predict the future action. This model leverages the idea of predictive coding [184] in the form of next feature prediction as an auxiliary task to the main supervised early action classification. Generative models for video also tend to use adversarial [114], [115] losses. The work of [71] proposes the *cross-modal cycle-consistency* loss so that samples from one modality can be unequivocally mapped into a sample from the other modality and then back to the original one. The loss aims to minimize the distance between the original position and the final position after cycling back and is computed for all input clips/sentences in both directions. The work of [177] pre-train their model on a MTP task by means of feature regression through MSE. The resulting features are binarized through a hashing layer and fed to a clustering k-means algorithm. Similar to [64], they also point that samples near the boundary between clusters are the most informative, as they are not too similar nor too dissimilar to any given anchor. Sampling those points is given a higher probability. Finally, they also employ a cluster alignment task to learn more discriminative binary codes. Given the clusters, the network is retrained from scratch using all objectives. Interestingly, [14] proposes a training schedule which iteratively samples one semi-supervised task per batch. They find that retrieval results improve as more tasks are added to this setting.

3.4.3 Discussion on training strategies

There is extensive literature pointing towards the need for large-scale pre-training or strong regularization for training Transformers. In video literature, however, leveraging pre-trained backbones and using rather small Transformers seems to work well. We hypothesize that large CNN backbones and Transformers may be a key tandem: the former helping the later trump inductive biases, while Transformers provide the already well performing CNNs with long-range modeling of the learned features.

VTs are generally trained using supervised losses. It is more common to find uses of self-supervised video losses in multi-modal settings. Probably due to the success of BERT, models inheriting from it extend its tasks to video. When it comes to the choice of video only self-supervised tasks, there is a very limited spectrum to choose from in the current literature. Aside from few exceptions [14], [80], [177], works are limited to the use of contrastive losses, in particular InfoNCE.

4 APPLICATION TO VIDEO CLASSIFICATION

The task of video classification has attracted the most research in transformers for video given the generality of the task and the availability of large datasets for training and evaluation, allowing for a more comprehensive performance analysis later in Sec. 4.1. For details on VTs applied to other video-related tasks we refer the reader to Sec. S2.

Regarding video classification, few works rely on pure Transformers [9], [11], [12], [49], [90] that for the most part focus on efficiency: both [11] and [9] test various space-time decompositions, whereas [11] also tests tokenization strategies (2D vs 3D patches). They found that a pre-trained ViT [7] encoding 2D patches with a temporal encoder on top performed the best. The works of [12] and [90] propose different types of restricted attention: the former restricts locally in shifting windows and the latter by only attending to previous frame’s patches after having exchanged information with another efficient attention mechanism [156]. In [48] they opt for 3D patches whose receptive field is enlarged across stages by subsequently merging token embeddings. Others pursue building very deep Transformers by maintaining a very compact latent representation [130]. These larger Transformers for classification require large labeled datasets for fully-supervised training [12], [48] or heavily rely on self-supervised pre-training [50], [64]. For multi-modal datasets, encoder fusion [50] or hierarchical encoder fusion is utilized [65].

Several other works rely on larger (usually CNN-based) backbones [50], [64], [65], [76], [91], [93], [95], [97], facilitating the training on smaller datasets. When equipped with these backbones, shallow encoders can serve as mere pooling operators [76], [86], [95], [97]. For detection backbones, Transformers are also a natural way to fuse information among detections [98] or to allow them to attend over a larger visual context [10]. Although mostly used in pure Transformers, efficient designs have been explored for this kind of works as well, e.g. weight sharing [64].

4.1 Performance comparison on video classification

The majority of VTs designed for classification are evaluated on manually annotated action recognition datasets that are

	Ref.	Name	Input	TF $\times (v_t \times v_s)$	MP.	Pre-train	Acc.
3D CNNs	[94]	R(2+1)D-34	32 x 112 ²	0.15 x (10 x 1)	64	-	72.0 / 90.0
	[87]	I3D	64 x 224 ²	0.11 x NA	12	IN-1K	72.1 / 90.3
	[83]	SF 16x8 R101+NL	16 x 256 ²	0.23 x (10 x 3)	60	-	79.8 / 93.9
	[185]	X3D-XXL	16 x 312 ²	0.19 x (10 x 3)	20	-	80.4 / 94.6
	[15]	NL R101	128 x 224 ²	0.36 x (10 x 1)	54	IN-1K	77.7 / 93.3
Transformers	[48]	MViT-S	16 x 224 ²	0.03 x (5 x 1)	26	-	76.0 / 92.1
		MViT-B 16x4	16 x 224 ²	0.07 x (5 x 1)	37	-	78.4 / 93.5
		MViT-B 32x3	32 x 224 ²	0.17 x (5 x 1)	37	-	80.2 / 94.4
		MViT-B 64x4	64 x 224 ²	0.46 x (3 x 3)	37	-	81.2 / 95.1
		MViT-B 32x3	32 x 224 ²	0.24 x (5 x 1)	53	-	-
	[90]	SCT-S	24 x 224 ²	0.09 x (4 x 3)	18.7	IN-21K	78.4 / 93.8
		SCT-M	24 x 224 ²	0.16 x (4 x 3)	33	IN-21K	81.3 / 94.5
		SCT-L	24 x 224 ²	0.34 x (4 x 3)	60	IN-21K	83.0 / 95.4
	[12]	Swin-T-1K	32 x 224 ²	0.09 x (4 x 3)	28	IN-1K	78.8 / 93.6
		Swin-S-1K	32 x 224 ²	0.17 x (4 x 3)	50	IN-1K	80.6 / 94.5
		Swin-B-1K	32 x 224 ²	0.28 x (4 x 3)	88	IN-1K	80.6 / 94.6
		Swin-B	32 x 224 ²	0.28 x (4 x 3)	88	IN-21K	82.7 / 95.5
		Swin-L	32 x 224 ²	0.60 x (4 x 3)	197	IN-21K	83.1 / 95.9
		Swin-L-384	32 x 384 ²	2.11 x (4 x 3)	200	IN-21K	84.6 / 96.5
		Swin-L-384-10x5	32 x 384 ²	2.11 x (10 x 5)	200	IN-21K	84.9 / 96.7
	[9]	TS	8 x 224 ²	0.20 x (1 x 3)	121	IN-21K	78.0 / 93.7
		TS-HR	16 x 448 ²	1.70 x (1 x 3)	121	IN-21K	79.7 / 94.4
		TS-L	96 x 224 ²	2.38 x (1 x 3)	121	IN-21K	80.7 / 94.7
	[49]	VATT-B	32 x 320 ²	0.76 x (4 x 3)	88	AS+H100M*	79.6 / 94.9
		VATT-M	32 x 320 ²	1.25 x (4 x 3)	155	AS+H100M*	81.1 / 95.6
		VATT-L	32 x 320 ²	2.48 x (4 x 3)	306	AS+H100M*	82.1 / 95.5
		VATT-MA-M	32 x 320 ²	1.25 x (4 x 3)	155	AS+H100M*	79.9 / 94.9
	[11]	ViViT-L/16x2	32 x 224 ²	3.98 x (1 x 3)	352	IN-21K	81.7 / 93.8
ViViT-L/16x2 (JFT)		32 x 224 ²	3.98 x (1 x 3)	352	JFT	83.5 / 94.3	
ViViT-H/16x2 (JFT)		32 x 224 ²	3.98 x (4 x 3)	352	JFT	84.9 / 95.8	
[99]	VTN-1	250 x 224 ²	4.21 x (1 x 1)	96	IN-21K	78.6 / 93.4	
	VTN-3	250 x 224 ²	4.21 x (1 x 1)	114	IN-21K	78.6 / 93.7	
	VTN-3 (Aug)	250 x 224 ²	4.21 x (1 x 1)	114	IN-21K	79.8 / 94.2	

* Only a subset of HowTo100M (H100M) [148] used for training.

TABLE 2

Classification accuracy on Kinetics-400 (Top1 / Top5). "Input" = number of frames x spatial resolution², "TF" = TFLOPs/view, v_t = number of temporal clips, v_s = number of spatial crops, "MP" = millions of parameters.

	Ref.	Name	Input	TF $\times (v_t \times v_s)$	MP.	Backbone	Pre-train	U101	H51
P+L+E	[91]	CATE	32 x 224 ²	NA x (8 x 1)	45	SF-RN50	K400	84.3	53.6
	[65]	CBT	30 x 112 ²	NA x (1 x 1)	15	S3D	K400	54.0	29.5
	[49]	VATT-M+SVM	32 x 320 ²	125 x (4 x 3)	155	-	AS+H100M*	89.2	63.3
		VATT-M+LRC	32 x 320 ²	125 x (4 x 3)	155	-	AS+H100M*	89.6	65.2
		VATT-MA+LRC	32 x 320 ²	125 x (4 x 3)	155	-	AS+H100M*	84.4	63.1
P+F+E	[64]	PE (V-CNN)	16 x 128 ²	NA x (10 x 3)	31	SF-RN50	AS	86.1	-
	[91]	CATE	32 x 224 ²	NA x (8 x 1)	45	3D RN-50	K400	88.4	61.9
	[65]	CBT	30 x 112 ²	NA x (1 x 1)	15	S3D	K400	79.5	44.5
	[97]	STCA	90 x 112 ²	78 x (9 x 2)	42	R(2+1)D-18	K400	93.1	67.0
	[76]	LIT BERT (32f)	32 x 112 ²	153 x NA	67	R(2+1)D-34	IG65M	98.7	84.0
		LIT BERT (64f)	64 x 112 ²	NA x NA	67	R(2+1)D-34	IG65M	98.7	85.1
	[90]	SCT-S	24 x 224 ²	88 x (4 x 3)	19	-	K400*	98.3	81.5
		SCT-M	24 x 224 ²	163 x (4 x 3)	33	-	K400*	98.5	83.2
		SCT-L	24 x 224 ²	343 x (4 x 3)	60	-	K400*	98.7	84.6

TABLE 3

Classification accuracy on UCF101 and HMDB51. "Input" = number of frames x spatial resolution², "TF" = TFLOPs/view, v_t = number of temporal clips, v_s = number of spatial crops, "MP" = millions of parameters, "*" = subset of the data. The group of "P+F+E" also fine-tune in UCF101/HMDB51.

public, so as to be compared with other works fairly. We next see in which datasets these works chose to evaluate. Then, another important aspect to discuss is the evaluation protocol, tightly related to the training regime (see Sec. 3.4.1).

Datasets. Among action classification datasets, the most popular one is undoubtedly the large-scale *Kinetics-400* (K400) [146], consisting of 306K videos of 10 seconds duration and 400 manually annotated classes. Among smaller datasets, the most commonly used are UCF101 [186], which is composed of 13K videos belonging to 101 action categories, around ~ 7 seconds each; and HMDB51 [187], that includes 6.7K videos of ~ 3 seconds from 51 classes. Additional results on Kinetics-600 [188] and ImageNet, as well as a graphical visualization of K400 results, can be found in Sec. S3.

Evaluation protocols. We will be referring to them as: "training and evaluation" (T+E), the protocol that does both on the same dataset; "pre-training, fine-tuning, and

evaluation" (P+F+E) to the one using different datasets for pre-training and for fine-tuning and evaluation; and "pre-training, linear probing, and evaluation" (P+L+E) the one that skips fine-tuning most of the weights except for the final classification layer. We noticed T+E or P+F+E are followed when evaluating on large manually annotated datasets, whereas P+L+E (or, more rarely P+F+E) on the smaller ones.

4.1.1 Performance on K400

Large models usually conduct P+F+E on K400 by using the training set to train and the validation set to report Top1 and Top5 accuracy [9], [11], [12], [49], [90], [99]. ViViT [11], VideoSwin [12], TS [9], SCT [90], and VTN [99] pre-train on ImageNet-1K/21K, whereas ViViT also experiments going bigger with the a private dataset, namely JFT. Meanwhile, VATT [11] exploits its multi-modality by pre-training in AudioSet (AS) and HowTo100M (H100M). Differently from all of them, [48] trains from scratch in K400 in a T+E evaluation scheme.

In Tab. 2, we can observe the best performing among all the models are "Swin-L-384-10x5" and "ViViT-H (JFT)" both reaching 84.9% Top1. "ViViT-H (JFT)" places second only because a lower Top5 score (95.8% vs. 96.7%). Besides performance, "ViViT-H (JFT)" inconveniently relies on heavier pre-training (JFT instead of ImageNet-21K) and has more parameters ($\times 1.76$), whereas "Swin-L-384-10x5" has the drawback of doubling the number of TFLOPs with respect to the ViViT competitor due to using 50 clips/video instead of 12. Nonetheless, "Swin-L-384" is able to compete with the former two (84.6% Top1), matching that of "ViViT-H (JFT)" while bringing down the number of TFLOPs by 25% and 50%, compared to ViViT and its "10x5" own variant respectively. At a considerable distance, "ViViT-L" (81.7%) points out the contribution of JFT pre-training in ViViT. In fact, a smaller "Swin-B" (82.7%) surpasses most larger models, not only in terms of TFLOPs ("MViT-B 64x4", "TS-L", and all VATT variants) but also parameters ("TS-HR"). The only exception being "SCT-L" (83.0%) that achieves marginally better results than "Swin-B" with 32% less parameters, slightly increasing in TFLOPs ($\times 1.21$). In general, SCT seems to be more cost-effective than Swin. On its turn, VTN requires approximately the same TFLOPs/view as ViViT despite having around a third of the parameters, but obtains lower accuracies than ViViT or even than the much more lightweight MViT-B. Regarding efficiency, MViT is a clear winner at the expense of performance (81.2% by "MViT-B 64x4" being its best result); MViT performs similarly to TS with fewer TFLOPs and much less parameters. TS and VATT, despite being rather heavy models, perform worse than others. More specifically, VATT-L (82.1%) does better than any MViT, but with a cost that is comparable to larger Swin and ViViT models. Note VATT was designed to generalize across different multi-modal tasks, not particularly for video classification. VATT also happens to use frame tokenization and, hence, could be limited when spatially attending to objects in the videos that are relevant for the actions trying to be classified. All in all, we observe a clear correlation between the size of the models and their performance, in addition to the well-known correlation between the number of views and performance [189].

Comparison to 3D ConvNets. Until recently, 3D CNNs (and their factorized space-time variants) have dominated the state-of-the-art of video classification. For the sake of completeness, Tab. 2 comprises several of them, to illustrate how VTs have surpassed them, with a +4.5% accuracy when comparing best models of each kind (“Swin-L-384-10x5” vs. “X3D-XXL”). Even when considering cost-effectiveness, “SCT-L” outperforms “SlowFast 16x8 R101+NL” by +3.2% with the same number of parameters and less TFLOPs (-41%). “Swin-B” also performs better with marginally more parameters than equivalently-sized CNN models.

4.1.2 Performance on UCF101 and HMDB51

There are also works leveraging smaller datasets to evaluate the generalization of their models, thus following either P+L+E or P+F+E evaluations. The evaluation of these models is depicted in Tab. 3. Among the models already discussed, only SCT and VATT are evaluated on UCF101 and HMDB51. In particular, “VATT-M+LRC” obtains an accuracy of 89.6% on UCF101 pre-training on AS and H100M, while “SCT-L” reaches a much higher 98.7% by pre-training on K400. Also on HMDB51, “VATT-M+LRC” scores much lower (65.2%) than “SCT-L” (84.6%). We hypothesize linear probing might not be enough to adapt general multi-modal models such as VATT.

LTT [76] is the only work sticking to P+F+E that uses the Transformer during inference. Their approach scores 98.7% on UCF101 and 85.1% on HMDB51, despite using a very shallow Transformer. These results prove the feasibility of fine-tuning VTs also in smaller datasets. Interestingly, there is a line of works that entirely remove the Transformer at evaluation time, which serves only to learn representations in their respective backbones. STiCA [97] (93.1% on UCF101 and 67.0% on HMDB51) is the one that performs the best, followed by CATE [91] (88.4% and 61.9%). PE (V-CNN) [64] is only evaluated in UCF-101 (86.1%), whereas CBT [65] performs the worst among these. There are two key differences that could explain the gap: opposed to CATE, PE (V-CNN) and CBT do not train with spatiotemporal augmentations and were designed for multi-task and multi-modal settings.

5 DISCUSSION

In this work we have comprehensively analysed how the field of Computer Vision has adapted Transformers to model video data. Given the inherent limitations of Transformers and the great complexity and dimensionality of videos, most changes focus on handling the computational burden. This is done transversally across many stages of the Transformer pipeline.

Using large CNNs on their own has proven well performant for video tasks (see Sec. 4.1.1). When used as backbones for VTs, they provide useful representations thanks to their inductive biases while performing dimensionality reduction. The Transformer can then focus on learning long-range interactions and further boost performance. As we have seen, training end-to-end this backbone and Transformer tandem may be essential. Another key element which explicitly tackles Transformer limitations for video are efficient designs. The two main approaches present in the literature so far are to decompose all-to-all attention into several smaller attention operations or progressively

aggregating information across layers. Aside from aiding efficiency, these approaches also bias the Transformer to separately focus on different types of features (e.g., spatial first, then temporal), which helps find a better balance between computation and performance [9], [11]. Another way in which the reviewed works explicitly exploit the structure of video is through tokenization. For this we find new strategies specific for this kind of data, such as frames or clips for modeling long-range temporal interactions, but also patches when a more fine-grained spatiotemporal interaction of the data is needed.

Finally, most video works train in a supervised fashion, directly on downstream tasks. However, more than a third of VT works have leveraged multi-modal information as additional cues to learn video representations. These additional modalities help provide relevant cues for learning video without requiring supervision. For this reason, in most of these cases we find the use of a self-supervised loss that aids to exploit those cues. While some of these losses have been adapted from the widely used BERT, it is also quite common to find contrastive approaches as an alternative. This can further alleviate the need for larger manually annotated sets of data in order for the Transformer to learn video representations.

5.1 The road ahead

VTs are still in its infancy and despite seeing clear trends, much more research is needed. Next we point out some of the research directions we deem relevant seen the current state of the field.

Training regime. Most non-video Transformer literature points towards large-scale self-supervised pre-training as a key element for proper learning [2], [7], [165]. In spite of that, most VTs are still fully supervised. This could be explained by the use of large CNN backbone networks, which are not so common in other fields, such as NLP. In fact, some video works have explicitly leveraged Transformer layers for training backbone networks [64], [65], [91], which points towards Transformers providing CNNs with useful long-range based feedback when trained end-to-end. Nevertheless, to the best of our knowledge, no empirical study has yet been conducted thoroughly analysing the contribution of all modules and training stages involved in visual Transformers.

Furthermore, self-supervised approaches are mostly limited to contrastive techniques, while there are a plethora of video self-supervised tasks yet to be tested on VTs. Some examples include temporal consistency [190], [191], inter-frame predictability [192], geometric transformations [193], motion statistics [194] or playback speed [195], [196]. Moreover, there has been a recent surge of self-supervised vision tasks, such as SimCLR [182] and Barlow Twins [197] for images or BraVe [198] for video. Some such method, DINO [199], has achieved impressive results for image Transformers.

Relative Positional Encodings. We do not find much novelty regarding positional encodings for video. Most approaches still follow image works, dominated by absolute PEs, but we see great promise in the use of relative PEs for video. Given its inherent capability to generalize to unseen lengths, VTs could greatly benefit from them.

Efficient designs. So far we find most works proposing to use some form of local or spatiotemporal decomposition, hierarchical designs and weight sharing. Nevertheless, we see a lot of promise in sparse approaches, given the huge redundancy of video data, which are not so common in VTs. In a similar fashion, video models could greatly benefit from longer time spans by leveraging memory modules (such as the one seen in [58]) to create recurrent Transformers and extend VTs receptive field even further. Using SA to update these modules could be key for better aggregating and exploiting past states. Also, a plethora of efficient Transformer architectures and strategies have been proposed by works in other modalities (for a complete overview see [19], [20]), such as network quantization [200], micro-batching [201] or Neural Architecture Search [202], which are yet to be explored for video models.

Application. Aside from very few exceptions, we see VTs applied to high level tasks only. Low-level tasks for video, such as frame generation [60], [61] or inpainting [114], [115], are much more challenging given the difficulty and computational complexity of generating low-level detail in a highly dimensional space. Still, we hypothesize that, when properly handled, the long-range modeling capabilities of Transformers could greatly benefit these tasks.

Inductive Biases. Beyond positional biases from PEs [167], some image-based works have proposed distilling them from pre-trained CNNs [166], [166], [203], which are promising research directions for infusing inductive spatiotemporal biases in VTs.

Explainability. Transformers provide a straightforward manner to peek into what they are paying attention to [204]. While this does not provide a deep understanding on the kind of relationships the model has learned [205], it yields some insights as to what it deems important for specific samples [206]. Few works have tried to interpret Transformers further than this for vision [207], and so far within the literature of VTs we only find a limited subset of works that visualize these attention activations for specific samples [66], [69], [99], [130]. The work of [14] consistently finds 6 different patterns in their cross-modal attention, showing, for instance, how some heads learn local, modality specific or cross-modal attention. In [104] they analyse the contribution of multiple experts to the final representation. The work of [97] shows how cropping augmentations helped the model learn audio sources tied to specific spatiotemporal regions of the video. Only [80] goes one step further and use rollout [208], which aggregates attention over multiple heads. As we can see, explainability of Transformers is still an open issue [209], which is also true for the video ones.

Generalization. While some works have studied the generalization capabilities of Transformers, it has been generally limited to NLP, such as out-of-distribution (OOD) generalization [210] or testing pre-trained language models in other modalities with minimal fine-tuning [211]. Regarding vision Transformers, to the best of our knowledge, only one work has studied in depth the topic of generalization [212], but we also find analysis on robustness of vision Transformers to different perturbations [213]. All these works have consistently found promising generalization capabilities of Transformer architectures. Nevertheless, VTs are still a mystery with regards to this, and are limited to few works

which have tested their model on OOD data [13], [62], [68], [69], [115], [126] or evaluated the learned features in other settings [50], [52], [71], [88]. While we expect them to follow the same trend as other modalities, further research is needed.

Future work. We have focused on analysing main trends, as well as relevant video specific Transformer design choices for most components of its pipeline. However, a more in depth analysis of performance capabilities of different efficient designs, as well as the merits of different training regimes is still required. A common benchmark and implementation for testing this variability across different Transformer stages is also needed. Furthermore, we long to see Transformer architectures compared with other non-local approaches for video understanding, as we see great promise in global-based learning techniques.

REFERENCES

- [1] A. Vaswani, N. Shazeer, N. Parmar, J. Uszkoreit, L. Jones, A. N. Gomez, L. u. Kaiser, and I. Polosukhin, "Attention is all you need," in *NeurIPS*, 2017. 1, 2, 3, 6
- [2] J. Devlin, M.-W. Chang, K. Lee, and K. Toutanova, "BERT: Pre-training of deep bidirectional transformers for language understanding," in *Computational Linguistics*, 2019. 1, 3, 4, 9, 10, 11, 15, 21
- [3] C. Plizzari, M. Cannici, and M. Matteucci, "Skeleton-based action recognition via spatial and temporal transformer networks," *CVIU*, 2021. 1
- [4] Y. Gong, Y.-A. Chung, and J. Glass, "AST: Audio Spectrogram Transformer," in *Interspeech*, 2021. 1
- [5] N. Parmar, A. Vaswani, J. Uszkoreit, L. Kaiser, N. Shazeer, A. Ku, and D. Tran, "Image transformer," in *ICML*, 2018. 1
- [6] P. Ramachandran, N. Parmar, A. Vaswani, I. Bello, A. Levskaya, and J. Shlens, "Stand-alone self-attention in vision models," in *NeurIPS*, 2019. 1, 11
- [7] A. Dosovitskiy, L. Beyer, A. Kolesnikov, D. Weissenborn, X. Zhai, T. Unterthiner, M. Dehghani, M. Minderer, G. Heigold, S. Gelly, J. Uszkoreit, and N. Houlsby, "An image is worth 16x16 words: Transformers for image recognition at scale," in *ICLR*, 2021. 1, 3, 4, 6, 7, 8, 10, 11, 13, 15
- [8] N. Carion, F. Massa, G. Synnaeve, N. Usunier, A. Kirillov, and S. Zagoruyko, "End-to-end object detection with transformers," in *ECCV*, 2020. 1, 5, 11
- [9] G. Bertasius, H. Wang, and L. Torresani, "Is space-time attention all you need for video understanding?" in *ICML*, 2021. 1, 3, 4, 5, 7, 11, 13, 14, 15, 21, 23, 24
- [10] R. Girdhar, J. Carreira, C. Doersch, and A. Zisserman, "Video action transformer network," in *CVPR*, 2019. 1, 3, 4, 5, 6, 7, 8, 11, 13, 22
- [11] A. Arnab, M. Dehghani, G. Heigold, C. Sun, M. Lucic, and C. Schmid, "Vivit: A video vision transformer," in *ICCV*, 2021. 1, 3, 4, 5, 7, 8, 11, 13, 14, 15, 21, 23, 24
- [12] Z. Liu, J. Ning, Y. Cao, Y. Wei, Z. Zhang, S. Lin, and H. Hu, "Video swin transformer," *arXiv*, 2021. 1, 3, 4, 5, 6, 7, 8, 11, 13, 14, 21, 23, 24
- [13] L. Zhu and Y. Yang, "Actbert: Learning global-local video-text representations," in *CVPR*, 2020. 1, 3, 4, 5, 6, 7, 9, 10, 12, 16, 21, 22
- [14] L. Li, Y.-C. Chen, Y. Cheng, Z. Gan, L. Yu, and J. Liu, "Hero: Hierarchical encoder for video+ language omni-representation pre-training," in *EMNLP*, 2020. 1, 3, 5, 6, 7, 8, 9, 10, 11, 12, 13, 16, 21, 22
- [15] X. Wang, R. Girshick, A. Gupta, and K. He, "Non-local neural networks," in *CVPR*, 2018. 1, 2, 14, 23, 24
- [16] A. Buades, B. Coll, and J.-M. Morel, "Non-local means denoising," *IPO*, 2011. 1
- [17] T. Lin, Y. Wang, X. Liu, and X. Qiu, "A survey of transformers," *arXiv*, 2021. 1
- [18] K. S. Kalyan, A. Rajasekharan, and S. Sangeetha, "AMMUS : A survey of transformer-based pretrained models in natural language processing," *arXiv*, 2021. 1
- [19] Y. Tay, M. Dehghani, D. Bahri, and D. Metzler, "Efficient transformers: A survey," *arXiv*, 2020. 1, 8, 16

- [20] Q. Fournier, G. M. Caron, and D. Aloise, "A practical survey on faster and lighter transformers," *arXiv*, 2021. **1, 8, 16**
- [21] S. Khan, M. Naseer, M. Hayat, S. W. Zamir, F. S. Khan, and M. Shah, "Transformers in vision: A survey," *arXiv*, 2021. **1, 10**
- [22] K. Han, Y. Wang, H. Chen, X. Chen, J. Guo, Z. Liu, Y. Tang, A. Xiao, C. Xu, Y. Xu, Z. Yang, Y. Zhang, and D. Tao, "A survey on vision transformer," *arXiv*, 2020. **1**
- [23] Y. Liu, Y. Zhang, Y. Wang, F. Hou, J. Yuan, J. Tian, Y. Zhang, Z. Shi, J. Fan, and Z. He, "A Survey of Visual Transformers," *arXiv*, 2021. **1**
- [24] Y. Xu, H. Wei, M. Lin, Y. Deng, K. Sheng, M. Zhang, F. Tang, W. Dong, F. Huang, and C. Xu, "Transformers in computational visual media: A survey," *Computational Visual Media*, 2022. **1**
- [25] A. Shin, M. Ishii, and T. Narihira, "Perspectives and prospects on transformer architecture for cross-modal tasks with language and vision," *arXiv*, 2021. **1**
- [26] L. Ruan and Q. Jin, "Survey: Transformer based video-language pre-training," *arXiv*, 2021. **1**
- [27] S. Cho, M. Maqbool, F. Liu, and H. Foroosh, "Self-attention network for skeleton-based human action recognition," in *WACV*, 2020. **1**
- [28] A. Tjandra, C. Liu, F. Zhang, X. Zhang, Y. Wang, G. Synnaeve, S. Nakamura, and G. Zweig, "Deja-vu: Double feature presentation and iterated loss in deep transformer networks," in *ICASSP*, 2020. **1**
- [29] D. Bahdanau, K. Cho, and Y. Bengio, "Neural machine translation by jointly learning to align and translate," in *ICLR*, 2015. **2**
- [30] S. Xiao, Z. Zhao, Z. Zhang, X. Yan, and M. Yang, "Convolutional hierarchical attention network for query-focused video summarization," in *AAAI*, 2020. **2**
- [31] W. Jin, Z. Zhao, M. Gu, J. Xiao, F. Wei, and Y. Zhuang, "Video dialog via progressive inference and cross-transformer," in *EMNLP-IJCNLP*, 2019. **2**
- [32] A. Bielski and T. Trzcinski, "Understanding multimodal popularity prediction of social media videos with self-attention," *IEEE Access*, 2018. **2**
- [33] P. Veličković, G. Cucurull, A. Casanova, A. Romero, P. Liò, and Y. Bengio, "Graph attention networks," in *ICML*, 2018. **2**
- [34] J. Zhang, X. Shi, J. Xie, H. Ma, I. King, and D. Yeung, "Gaan: Gated attention networks for learning on large and spatiotemporal graphs," in *Uncertainty in AI*, 2018. **2**
- [35] H. Hu, J. Gu, Z. Zhang, J. Dai, and Y. Wei, "Relation networks for object detection," in *CVPR*, 2018. **2**
- [36] Y. Chen, Y. Cao, H. Hu, and L. Wang, "Memory enhanced global-local aggregation for video object detection," in *CVPR*, 2020. **2**
- [37] X. Wang, X. Xiong, M. Neumann, A. Piergiovanni, M. S. Ryoo, A. Angelova, K. M. Kitani, and W. Hua, "Attentionnas: Spatiotemporal attention cell search for video classification," in *ECCV*, 2020. **2, 4**
- [38] C.-T. Liu, C.-W. Wu, Y.-C. F. Wang, S.-Y. Chien, and I. Center, "Spatially and temporally efficient non-local attention network for video-based person re-identification," in *BMVC*, 2019. **2**
- [39] Z. Wang, S. Luo, H. Sun, H. Pan, and J. Yin, "An efficient non-local attention network for video-based person re-identification," in *ICIT*, 2019. **2**
- [40] J. Fajtl, H. S. Sokeh, V. Argyriou, D. Monekosso, and P. Remagnino, "Summarizing videos with attention," in *ACCV*, 2018. **2, 5, 6, 11, 21**
- [41] A. Johnston and G. Carneiro, "Self-supervised monocular trained depth estimation using self-attention and discrete disparity volume," in *CVPR*, 2020. **2, 4**
- [42] J. Yin, J. Shen, C. Guan, D. Zhou, and R. Yang, "Lidar-based online 3d video object detection with graph-based message passing and spatiotemporal transformer attention," in *CVPR*, 2020. **2, 5, 7, 8, 11, 22**
- [43] J. L. Ba, J. R. Kiros, and G. E. Hinton, "Layer normalization," *NeurIPS*, 2016. **2**
- [44] I. O. Tolstikhin, N. Houlsby, A. Kolesnikov, L. Beyer, X. Zhai, T. Unterthiner, J. Yung, D. Keysers, J. Uszkoreit, M. Lucic, and A. Dosovitskiy, "Mlp-mixer: An all-mlp architecture for vision," *arXiv*, 2021. **2**
- [45] J. Lee-Thorp, J. Ainslie, I. Eckstein, and S. Ontanon, "Fnet: Mixing tokens with fourier transforms," *arXiv*, 2021. **2**
- [46] Y. Dong, J.-B. Cordonnier, and A. Loukas, "Attention is not all you need: pure attention loses rank doubly exponentially with depth," in *ICML*, 2021. **2**
- [47] A. Radford, K. Narasimhan, T. Salimans, and I. Sutskever, "Improving language understanding by generative pre-training," in *OpenAI Preprint*, 2018. **3**
- [48] H. Fan, B. Xiong, K. Mangalam, Y. Li, Z. Yan, J. Malik, and C. Feichtenhofer, "Multiscale vision transformers," in *ICCV*, 2021. **3, 4, 5, 6, 7, 11, 13, 14, 21, 23, 24**
- [49] H. Akbari, L. Yuan, R. Qian, W.-H. Chuang, S.-F. Chang, Y. Cui, and B. Gong, "Vatt: Transformers for multimodal self-supervised learning from raw video, audio and text," *arXiv*, 2021. **3, 4, 5, 6, 7, 8, 11, 12, 13, 14, 21, 22, 23, 24**
- [50] C. Sun, A. Myers, C. Vondrick, K. Murphy, and C. Schmid, "Videobert: A joint model for video and language representation learning," in *ICCV*, 2019. **3, 5, 6, 7, 9, 11, 12, 13, 16, 21, 22**
- [51] A. Miech, J.-B. Alayrac, I. Laptev, J. Sivic, and A. Zisserman, "Thinking fast and slow: Efficient text-to-visual retrieval with transformers," in *CVPR*, 2021. **3, 5, 10, 11, 12, 21, 22**
- [52] J. Tan, J. Tang, L. Wang, and G. Wu, "Relaxed transformer decoders for direct action proposal generation," in *ICCV*, 2021. **3, 5, 6, 10, 11, 16, 21, 22**
- [53] M. Zhang, Y. Yang, X. Chen, Y. Ji, X. Xu, J. Li, and H. T. Shen, "Multi-stage aggregated transformer network for temporal language localization in videos," in *CVPR*, 2021. **3, 5, 6, 10, 11, 12, 21, 22**
- [54] V. Iashin and E. Rahtu, "A better use of audio-visual cues: Dense video captioning with bi-modal transformer," in *BMVC*, 2020. **3, 5, 9, 10, 11, 21, 22**
- [55] K.-M. Kim, S.-H. Choi, J.-H. Kim, and B.-T. Zhang, "Multimodal dual attention memory for video story question answering," in *ECCV*, 2018. **3, 5, 7, 8, 9, 10, 11, 21, 23**
- [56] V. Iashin and E. Rahtu, "Multi-modal dense video captioning," in *CVPR*, 2020. **3, 5, 9, 10, 11, 21, 22**
- [57] L. Zhou, Y. Zhou, J. J. Corso, R. Socher, and C. Xiong, "End-to-end dense video captioning with masked transformer," in *CVPR*, 2018. **3, 5, 6, 10, 11, 21, 22**
- [58] J. Lei, L. Wang, Y. Shen, D. Yu, T. L. Berg, and M. Bansal, "Mart: Memory-augmented recurrent transformer for coherent video paragraph captioning," in *ACL*, 2020. **3, 4, 5, 6, 7, 8, 9, 10, 11, 16, 22**
- [59] Z. Yu and N. Han, "Accelerated masked transformer for dense video captioning," *Neurocomputing*, 2021. **3, 5, 6, 10, 11, 22**
- [60] D. Weissenborn, O. Täckström, and J. Uszkoreit, "Scaling autoregressive video models," in *ICLR*, 2020. **3, 5, 6, 7, 11, 16, 21, 22**
- [61] R. Rakhimov, D. Volkhonskiy, A. Artemov, D. Zorin, and E. Burnaev, "Latent video transformer," *arXiv*, 2020. **3, 5, 6, 7, 16, 22**
- [62] W. Weng, Y. Zhang, and Z. Xiong, "Event-based video reconstruction using transformer," in *ICCV*, 2021. **3, 4, 5, 8, 11, 16, 22**
- [63] H. Zhou, A. Kadav, F. Lai, A. Niculescu-Mizil, M. R. Min, M. Kapadia, and H. P. Graf, "Hopper: Multi-hop transformer for spatiotemporal reasoning," in *ICLR*, 2021. **3, 5, 10, 11, 22**
- [64] S. Lee, Y. Yu, G. Kim, T. Breuel, J. Kautz, and Y. Song, "Parameter efficient multimodal transformers for video representation learning," in *ICLR*, 2021. **3, 5, 6, 7, 8, 9, 11, 12, 13, 14, 15, 21, 22**
- [65] C. Sun, F. Baradel, K. Murphy, and C. Schmid, "Contrastive bidirectional transformer for temporal representation learning," *arXiv*, 2019. **3, 4, 5, 6, 9, 12, 13, 14, 15, 21**
- [66] A. Pashevich, C. Schmid, and C. Sun, "Episodic transformer for vision-and-language navigation," in *ICCV*, 2021. **3, 4, 5, 6, 9, 11, 16, 23**
- [67] X. Wang, S. Zhang, Z. Qing, Y. Shao, Z. Zuo, C. Gao, and N. Sang, "Oadtr: Online action detection with transformers," in *ICCV*, 2021. **3, 5, 6, 11, 23**
- [68] J. Shao, X. Wen, B. Zhao, and X. Xue, "Temporal context aggregation for video retrieval with contrastive learning," in *WACV*, 2021. **3, 5, 12, 13, 16, 21, 22**
- [69] M. Patrick, P.-Y. Huang, Y. Asano, F. Metze, A. G. Hauptmann, J. F. Henriques, and A. Vedaldi, "Support-set bottlenecks for video-text representation learning," in *ICLR*, 2021. **3, 5, 6, 7, 9, 11, 13, 16, 21, 22**
- [70] S. Liu, H. Fan, S. Qian, Y. Chen, W. Ding, and Z. Wang, "Hit: Hierarchical transformer with momentum contrast for video-text retrieval," in *ICCV*, 2021. **3, 5, 9, 12, 13, 21, 22**
- [71] S. Ging, M. Zolfaghari, H. Pirsiavash, and T. Brox, "Coot: Co-operative hierarchical transformer for video-text representation learning," in *NeurIPS*, 2020. **3, 5, 6, 7, 8, 12, 13, 16, 21, 22**
- [72] J. Chen and H. Chao, "Videotrm: Pre-training for video captioning challenge 2020," in *ACM-MM*, 2020. **3, 11**

- [73] K. Wu, H. Peng, M. Chen, J. Fu, and H. Chao, "Rethinking and improving relative position encoding for vision transformer," in *ICCV*, 2021. 3, 6
- [74] A. Parikh, O. Täckström, D. Das, and J. Uszkoreit, "A decomposable attention model for natural language inference," in *Empirical Methods in Natural Language Processing*, 2016. 3, 6
- [75] D. Hendrycks and K. Gimpel, "Gaussian error linear units (gelus)," *arXiv*, 2016. 3
- [76] M. E. Kalfaoglu, S. Kalkan, and A. A. Alatan, "Late temporal modeling in 3d cnn architectures with bert for action recognition," in *ECCV*, 2020. 3, 5, 6, 9, 10, 11, 13, 14, 15
- [77] A. Baevski and M. Auli, "Adaptive input representations for neural language modeling," in *ICLR*, 2018. 3
- [78] N. C. Camgoz, O. Koller, S. Hadfield, and R. Bowden, "Sign language transformers: Joint end-to-end sign language recognition and translation," in *CVPR*, 2020. 3, 5, 10, 11, 23
- [79] R. Xiong, Y. Yang, D. He, K. Zheng, S. Zheng, C. Xing, H. Zhang, Y. Lan, L. Wang, and T. Liu, "On layer normalization in the transformer architecture," in *ICML*, 2020. 3
- [80] R. Girdhar and K. Grauman, "Anticipative video transformer," in *ICCV*, 2021. 3, 4, 5, 6, 7, 8, 11, 13, 16, 21, 23
- [81] R. R. A. Pramono, Y.-T. Chen, and W.-H. Fang, "Hierarchical self-attention network for action localization in videos," in *CVPR*, 2019. 3, 5, 7, 8, 11, 22
- [82] N. Wang, W. Zhou, J. Wang, and H. Li, "Transformer meets tracker: Exploiting temporal context for robust visual tracking," in *CVPR*, 2021. 3, 4, 5, 7, 8, 11, 21, 22
- [83] C. Feichtenhofer, H. Fan, J. Malik, and K. He, "Slowfast networks for video recognition," in *ICCV*, 2019. 5, 14, 23, 24
- [84] K. He, X. Zhang, S. Ren, and J. Sun, "Deep residual learning for image recognition," in *CVPR*, 2016. 5
- [85] S. Xie, C. Sun, J. Huang, Z. Tu, and K. Murphy, "Rethinking spatiotemporal feature learning for video understanding," *ECCV*, 2017. 4, 5
- [86] D. Purwanto, R. Renanda Adhi Pramono, Y.-T. Chen, and W.-H. Fang, "Extreme low resolution action recognition with spatial-temporal multi-head self-attention and knowledge distillation," in *CVPR*, 2019. 4, 5, 9, 11, 13
- [87] J. Carreira and A. Zisserman, "Quo vadis, action recognition? a new model and the kinetics dataset," in *CVPR*, 2017. 4, 5, 14, 23, 24
- [88] B. Yu, W. Li, X. Li, J. Lu, and J. Zhou, "Frequency-aware spatiotemporal transformers for video inpainting detection," in *ICCV*, 2021. 4, 5, 6, 11, 16, 22
- [89] S. Ren, K. He, R. Girshick, and J. Sun, "Faster r-cnn: Towards real-time object detection with region proposal networks," in *NeurIPS*, 2015. 4, 5
- [90] X. Zha, W. Zhu, L. Xun, S. Yang, and J. Liu, "Shifted chunk transformer for spatio-temporal representational learning," *NeurIPS*, 2021. 5, 7, 8, 11, 13, 14, 23, 24
- [91] C. Sun, A. Nagrani, Y. Tian, and C. Schmid, "Composable augmentation encoding for video representation learning," in *ICCV*, 2021. 5, 11, 12, 13, 14, 15
- [92] S. Kondo, "Lapformer: surgical tool detection in laparoscopic surgical video using transformer architecture," *Computer Methods in Biomechanics and Biomedical Engineering: Imaging and Visualization*, 2020. 4, 5, 11, 22
- [93] T. Perrett, A. Masullo, T. Burghardt, M. Mirmehdi, and D. Damen, "Temporal-relational crosstransformers for few-shot action recognition," in *CVPR*, 2021. 5, 6, 11, 13
- [94] D. Tran, H. Wang, L. Torresani, J. Ray, Y. LeCun, and M. Paluri, "A closer look at spatiotemporal convolutions for action recognition," in *CVPR*, 2018. 5, 14, 23, 24
- [95] K. Gavriluyk, R. Sanford, M. Javan, and C. G. Snoek, "Actor-transformers for group activity recognition," in *CVPR*, 2020. 4, 5, 6, 9, 10, 11, 13
- [96] J. Wang, K. Sun, T. Cheng, B. Jiang, C. Deng, Y. Zhao, D. Liu, Y. Mu, M. Tan, X. Wang *et al.*, "Deep high-resolution representation learning for visual recognition," *TPAMI*, 2020. 5
- [97] M. Patrick, P.-Y. Huang, I. Misra, F. Metze, A. Vedaldi, Y. M. Asano, and J. a. F. Henriques, "Space-time crop & attend: Improving cross-modal video representation learning," in *ICCV*, 2021. 5, 11, 12, 13, 14, 15, 16, 21, 22
- [98] S. Li, Q. Cao, L. Liu, K. Yang, S. Liu, J. Hou, and S. Yi, "Groupformer: Group activity recognition with clustered spatial-temporal transformer," in *ICCV*, 2021. 5, 13
- [99] D. Neimark, O. Bar, M. Zohar, and D. Asselmann, "Video transformer network," in *ICCV*, 2021. 5, 7, 8, 14, 16, 23, 24
- [100] S. Ioffe and C. Szegedy, "Batch normalization: Accelerating deep network training by reducing internal covariate shift," in *ICML*, 2015. 5
- [101] Z. Li, Z. Li, J. Zhang, Y. Feng, and J. Zhou, "Bridging text and video: A universal multimodal transformer for audio-visual scene-aware dialog," *IEEE/ACM TASLP*, 2021. 4, 5, 9, 10, 11, 21
- [102] J. Hu, L. Shen, and G. Sun, "Squeeze-and-excitation networks," in *CVPR*, 2018. 5
- [103] S. Xie, R. Girshick, P. Dollár, Z. Tu, and K. He, "Aggregated residual transformations for deep neural networks," in *CVPR*, 2017. 5
- [104] V. Gabeur, C. Sun, K. Alahari, and C. Schmid, "Multi-modal Transformer for Video Retrieval," in *ECCV*, 2020. 4, 5, 6, 7, 9, 11, 13, 16, 21, 22
- [105] G. Huang, Z. Liu, L. Van Der Maaten, and K. Q. Weinberger, "Densely connected convolutional networks," in *CVPR*, 2017. 5
- [106] A. Gordo, J. Almazan, J. Revaud, and D. Larlus, "End-to-end learning of deep visual representations for image retrieval," *ICCV*, 2017. 5
- [107] G. Kordopatis-Zilos, S. Papadopoulos, I. Patras, and I. Kompatsiaris, "Visil: Fine-grained spatio-temporal video similarity learning," in *ICCV*, 2019. 5
- [108] M. Dzabraev, M. Kalashnikov, S. Komkov, and A. Petiushko, "Mdmmt: Multidomain multimodal transformer for video retrieval," in *CVPR*, 2021. 5, 7, 13, 22
- [109] A. Radford, J. W. Kim, C. Hallacy, A. Ramesh, G. Goh, S. Agarwal, G. Sastry, A. Askell, P. Mishkin, J. Clark *et al.*, "Learning transferable visual models from natural language supervision," *arXiv*, 2021. 5
- [110] J. Lin, C. Gan, and S. Han, "Tsm: Temporal shift module for efficient video understanding," in *ICCV*, 2019. 5
- [111] B. Yu, M. Tang, L. Zheng, G. Zhu, J. Wang, H. Feng, X. Feng, and H. Lu, "High-performance discriminative tracking with transformers," in *ICCV*, 2021. 5, 21, 22
- [112] X. Chen, B. Yan, J. Zhu, D. Wang, X. Yang, and H. Lu, "Transformer tracking," in *CVPR*, 2021. 5, 11, 21, 22
- [113] B. Yan, H. Peng, J. Fu, D. Wang, and H. Lu, "Learning spatio-temporal transformer for visual tracking," in *ICCV*, 2021. 5, 22
- [114] Y. Zeng, J. Fu, and H. Chao, "Learning joint spatial-temporal transformations for video inpainting," in *ECCV*, 2020. 4, 5, 6, 11, 13, 16, 22
- [115] R. Liu, H. Deng, Y. Huang, X. Shi, L. Lu, W. Sun, X. Wang, J. Dai, and H. Li, "Fuseformer: Fusing fine-grained information in transformers for video inpainting," in *ICCV*, 2021. 4, 5, 11, 13, 16, 22
- [116] A. v. d. Oord, O. Vinyals, and K. Kavukcuoglu, "Neural discrete representation learning," *arXiv*, 2017. 5
- [117] R. Su, Q. Yu, and D. Xu, "Stvgbert: A visual-linguistic transformer based framework for spatio-temporal video grounding," in *ICCV*, 2021. 4, 5, 7, 10, 11, 22
- [118] D. Tran, L. Bourdev, R. Fergus, L. Torresani, and M. Paluri, "Learning spatiotemporal features with 3d convolutional networks," in *ICCV*, 2015. 5
- [119] Y. Gu, L. Wang, Z. Wang, Y. Liu, M.-M. Cheng, and S.-P. Lu, "Pyramid constrained self-attention network for fast video salient object detection," in *AAAI*, 2020. 4, 5, 7, 11, 21, 22
- [120] A. Howard, M. Sandler, G. Chu, and L.-C. e. a. Chen, "Searching for mobilenetv3," in *CVPR*, 2019. 5
- [121] Z. Yuan, X. Song, L. Bai, Z. Wang, and W. Ouyang, "Temporal-channel transformer for 3d lidar-based video object detection for autonomous driving," *T. Circuits and Systems for Video Technology*, 2021. 5
- [122] Y. Wang, Z. Xu, X. Wang, C. Shen, B. Cheng, H. Shen, and H. Xia, "End-to-end video instance segmentation with transformers," in *CVPR*, 2021. 4, 5, 6, 21, 22
- [123] Y. Wang, Z. Liu, Y. Xia, C. Zhu, and D. Zhao, "Spatiotemporal module for video saliency prediction based on self-attention," *Image and Vision Computing*, 2021. 4, 5, 6, 11, 22
- [124] L. Ye, M. Rochan, Z. Liu, X. Zhang, and Y. Wang, "Referring segmentation in images and videos with cross-modal self-attention network," *arXiv*, 2021. 5, 6, 22
- [125] L.-C. Chen, G. Papandreou, I. Kokkinos, K. Murphy, and A. L. Yuille, "DeepLab: Semantic image segmentation with deep convolutional nets, atrous convolution, and fully connected crfs," *TPAMI*, 2017. 5

- [126] Y.-T. Liu, Y.-J. Li, F.-E. Yang, S.-F. Chen, and Y.-C. F. Wang, "Learning hierarchical self-attention for video summarization," in *ICIP*, 2019. [4](#), [5](#), [16](#), [21](#), [22](#)
- [127] C. Szegedy, W. Liu, Y. Jia, P. Sermanet, S. Reed, D. Anguelov, D. Erhan, V. Vanhoucke, and A. Rabinovich, "Going deeper with convolutions," in *CVPR*, 2015. [5](#)
- [128] J. Lin and S.-h. Zhong, "Bi-directional self-attention with relative positional encoding for video summarization," in *ICTAI*, 2020. [5](#), [6](#), [11](#), [21](#), [22](#)
- [129] H. Seong, J. Hyun, and E. Kim, "Video multitask transformer network," in *ICCV*, 2019. [5](#), [7](#), [8](#)
- [130] A. Jaegle, F. Gimeno, A. Brock, A. Zisserman, O. Vinyals, and J. Carreira, "Perceiver: General perception with iterative attention," in *ICML*, 2021. [4](#), [5](#), [6](#), [7](#), [8](#), [9](#), [11](#), [13](#), [16](#), [21](#)
- [131] Y. Cong, W. Liao, H. Ackermann, B. Rosenhahn, and M. Y. Yang, "Spatial-temporal transformer for dynamic scene graph generation," in *ICCV*, 2021. [4](#), [5](#), [7](#), [23](#)
- [132] A. Prakash, K. Chitta, and A. Geiger, "Multi-modal fusion transformer for end-to-end autonomous driving," in *CVPR*, 2021. [5](#), [7](#), [8](#), [10](#), [11](#)
- [133] K. He, G. Gkioxari, P. Dollár, and R. Girshick, "Mask r-cnn," in *ICCV*, 2017. [5](#)
- [134] K. Fang, A. Toshev, L. Fei-Fei, and S. Savarese, "Scene memory transformer for embodied agents in long-horizon tasks," in *CVPR*, 2019. [5](#), [7](#), [9](#), [10](#), [23](#)
- [135] C. Szegedy, S. Ioffe, V. Vanhoucke, and A. A. Alemi, "Inception-v4, inception-resnet and the impact of residual connections on learning," in *AAAI*, 2017. [5](#)
- [136] N. C. Camgoz, O. Koller, S. Hadfield, and R. Bowden, "Multi-channel transformers for multi-articulatory sign language translation," in *ECCV*, 2020. [5](#), [9](#), [10](#), [11](#), [23](#)
- [137] M. Luo, S. Yang, X. Chen, Z. Liu, and S. Shan, "Synchronous bidirectional learning for multilingual lip reading," in *BMVC*, 2020. [5](#), [11](#), [23](#)
- [138] Y. Zhang, X. Li, C. Liu, B. Shuai, Y. Zhu, B. Brattoli, H. Chen, I. Marsic, and J. Tighe, "Vidtr: Video transformer without convolutions," in *ICCV*, 2021. [4](#), [5](#), [11](#), [23](#)
- [139] S. Li, X. Li, J. Lu, and J. Zhou, "Self-supervised video hashing via bidirectional transformers," in *CVPR*, 2021. [5](#), [22](#)
- [140] K. Simonyan and A. Zisserman, "Very deep convolutional networks for large-scale image recognition," *arXiv*, 2014. [5](#)
- [141] X. Chen, D. Liu, C. Lei, R. Li, Z.-J. Zha, and Z. Xiong, "Bert4essrec: Content-based video relevance prediction with bidirectional encoder representations from transformer," in *ACM-MM*, 2019. [5](#), [7](#), [11](#), [23](#)
- [142] D. Curto, A. Clapes, J. Selva, S. Smeureanu, J. C. S. J. Junior, D. Gallardo-Pujol, G. Guilera, D. Leiva, T. B. Moeslund, S. Escalera, and C. Palmero, "Dyadformer: A multi-modal transformer for long-range modeling of dyadic interactions," in *ICCV-W*, 2021. [5](#), [7](#), [8](#), [10](#), [23](#)
- [143] J. Deng, W. Dong, R. Socher, L.-J. Li, K. Li, and L. Fei-Fei, "ImageNet: A Large-Scale Hierarchical Image Database," in *CVPR*, 2009. [4](#)
- [144] T. Ridnik, E. Ben-Baruch, A. Noy, and L. Zelnik-Manor, "Imagenet-21k pretraining for the masses," in *NeurIPS*, 2021. [4](#), [11](#)
- [145] Y.-J. Heo, Y.-J. Choi, Y.-W. Lee, and B.-G. Kim, "Deepfake detection scheme based on vision transformer and distillation," *arXiv*, 2021. [4](#)
- [146] J. Carreira and A. Zisserman, "Quo vadis, action recognition? a new model and the kinetics dataset," in *CVPR*, 2017. [4](#), [14](#), [21](#), [23](#), [24](#)
- [147] J. Carreira, E. Noland, C. Hillier, and A. Zisserman, "A short note on the kinetics-700 human action dataset," *arXiv*, 2019. [4](#), [11](#)
- [148] A. Miech, D. Zhukov, J.-B. Alayrac, M. Tapaswi, I. Laptev, and J. Sivic, "Howto100m: Learning a text-video embedding by watching hundred million narrated video clips," in *ICCV*, 2019. [4](#), [11](#), [14](#), [24](#)
- [149] X. Shi, Z. Chen, H. Wang, D.-Y. Yeung, W.-k. Wong, and W.-c. Woo, "Convolutional lstm network: A machine learning approach for precipitation nowcasting," in *NeurIPS*, 2015. [4](#)
- [150] Z. Dai, Z. Yang, Y. Yang, J. G. Carbonell, Q. Le, and R. Salakhutdinov, "Transformer-xl: Attentive language models beyond a fixed-length context," in *ACL*, 2019. [6](#)
- [151] Z. Wu, Y. Xiong, S. X. Yu, and D. Lin, "Unsupervised feature learning via non-parametric instance discrimination," in *CVPR*, 2018. [6](#)
- [152] P. Shaw, J. Uszkoreit, and A. Vaswani, "Self-attention with relative position representations," in *NAACL*, 2018. [6](#)
- [153] I. Beltagy, M. E. Peters, and A. Cohan, "Longformer: The long-document transformer," *arXiv*, 2020. [7](#)
- [154] C. R. Qi, L. Yi, H. Su, and L. J. Guibas, "Pointnet++: Deep hierarchical feature learning on point sets in a metric space," *NeurIPS*, 2017. [7](#)
- [155] A. Andoni, P. Indyk, T. Laarhoven, I. Razenshteyn, and L. Schmidt, "Practical and optimal lsh for angular distance," in *NeurIPS*, 2015. [8](#)
- [156] N. Kitaev, L. Kaiser, and A. Levskaya, "Reformer: The efficient transformer," in *ICLR*, 2019. [8](#), [13](#)
- [157] L. Smith and M. Gasser, "The development of embodied cognition: Six lessons from babies," *Artificial Life*, 2005. [8](#)
- [158] A. Owens, J. Wu, J. H. McDermott, W. T. Freeman, and A. Torralba, "Ambient sound provides supervision for visual learning," in *ECCV*, 2016. [8](#)
- [159] J.-B. Alayrac, A. Recasens, R. Schneider, R. Arandjelović, J. Ramapuram, J. De Fauw, L. Smaira, S. Dieleman, and A. Zisserman, "Self-supervised multimodal versatile networks," in *NeurIPS*, 2020. [8](#)
- [160] A. Miech, J.-B. Alayrac, L. Smaira, I. Laptev, J. Sivic, and A. Zisserman, "End-to-end learning of visual representations from uncurated instructional videos," in *CVPR*, 2020. [9](#)
- [161] S. Hershey, S. Chaudhuri, and D. P. e. a. Ellis, "Cnn architectures for large-scale audio classification," in *ICASSP*, 2017. [9](#)
- [162] J. Lu, D. Batra, D. Parikh, and S. Lee, "Vilbert: Pretraining task-agnostic visiolinguistic representations for vision-and-language tasks," in *NeurIPS*, 2019. [10](#), [11](#)
- [163] K. Simonyan and A. Zisserman, "Two-stream convolutional networks for action recognition in videos," in *NeurIPS*, 2014. [10](#)
- [164] A. Radford, J. Wu, R. Child, D. Luan, D. Amodei, and I. Sutskever, "Language models are unsupervised multitask learners," in *OpenAI Blog*, 2019. [10](#)
- [165] X. Chen, C.-J. Hsieh, and B. Gong, "When vision transformers outperform resnets without pretraining or strong data augmentations," *arXiv*, 2021. [10](#), [15](#)
- [166] H. Touvron, M. Cord, M. Douze, F. Massa, A. Sablayrolles, and H. Jégou, "Training data-efficient image transformers & distillation through attention," in *ICML*, 2021. [10](#), [16](#)
- [167] Z. Dai, H. Liu, Q. V. Le, and M. Tan, "Coatnet: Marrying convolution and attention for all data sizes," in *NeurIPS*, 2021. [10](#), [11](#), [16](#)
- [168] A. Steiner, A. Kolesnikov, X. Zhai, R. Wightman, J. Uszkoreit, and L. Beyer, "How to train your vit? data, augmentation, and regularization in vision transformers," *arXiv*, 2021. [10](#)
- [169] Q. Xu, M. Zhang, Z. Gu, and G. Pan, "Overfitting remedy by sparsifying regularization on fully-connected layers of cnns," *Neurocomputing*, 2019. [11](#)
- [170] X. Zhai, A. Kolesnikov, N. Houlsby, and L. Beyer, "Scaling vision transformers," *arXiv*, 2021. [11](#)
- [171] D. Purwanto, R. R. A. Pramono, Y.-T. Chen, and W.-H. Fang, "Three-stream network with bidirectional self-attention for action recognition in extreme low resolution videos," *IEEE Signal Processing Letters*, 2019. [11](#)
- [172] C.-Y. Wu, C. Feichtenhofer, H. Fan, K. He, P. Krahenbuhl, and R. Girshick, "Long-term feature banks for detailed video understanding," in *CVPR*, 2019. [11](#)
- [173] Z. Yuan, X. Song, L. Bai, Z. Wang, and W. Ouyang, "Temporal-channel transformer for 3d lidar-based video object detection for autonomous driving," *Circuits and Systems for Video Technology*, 2021. [11](#), [22](#)
- [174] Y. Wang, Z. Xu, X. Wang, C. Shen, B. Cheng, H. Shen, and H. Xia, "End-to-end video instance segmentation with transformers," in *CVPR*, 2021. [11](#)
- [175] Z. Liu, Y. Lin, Y. Cao, H. Hu, Y. Wei, Z. Zhang, S. Lin, and B. Guo, "Swin transformer: Hierarchical vision transformer using shifted windows," *arXiv*, 2021. [11](#)
- [176] P. Sharma, N. Ding, S. Goodman, and R. Soicrut, "Conceptual captions: A cleaned, hypernymed, image alt-text dataset for automatic image captioning," in *Computational Linguistics*, 2018. [11](#)
- [177] S. Li, X. Li, J. Lu, and J. Zhou, "Self-supervised video hashing via bidirectional transformers," in *CVPR*, 2021. [11](#), [13](#)
- [178] M. Gutmann and A. Hyvärinen, "Noise-contrastive estimation: A new estimation principle for unnormalized statistical models," in *AISTATS*, 2010. [12](#)

- [179] A. v. d. Oord, Y. Li, and O. Vinyals, "Representation learning with contrastive predictive coding," *arXiv*, 2018. [12](#)
- [180] R. Jozefowicz, O. Vinyals, M. Schuster, N. Shazeer, and Y. Wu, "Exploring the limits of language modeling," *arXiv*, 2016. [12](#)
- [181] Y. Sun, C. Cheng, Y. Zhang, C. Zhang, L. Zheng, Z. Wang, and Y. Wei, "Circle loss: A unified perspective of pair similarity optimization," in *CVPR*, 2020. [12](#)
- [182] T. Chen, S. Kornblith, M. Norouzi, and G. Hinton, "A simple framework for contrastive learning of visual representations," in *ICML*, 2020. [12](#), [15](#)
- [183] K. He, H. Fan, Y. Wu, S. Xie, and R. Girshick, "Momentum contrast for unsupervised visual representation learning," in *CVPR*, 2020. [12](#)
- [184] R. P. Rao and D. H. Ballard, "Predictive coding in the visual cortex: a functional interpretation of some extra-classical receptive-field effects," *Nature Neuroscience*, 1999. [13](#)
- [185] C. Feichtenhofer, "X3d: Expanding architectures for efficient video recognition," in *CVPR*, 2020. [14](#), [23](#), [24](#)
- [186] K. Soomro, A. R. Zamir, and M. Shah, "Ucf101: A dataset of 101 human actions classes from videos in the wild," *arXiv*, 2012. [14](#)
- [187] H. Kuehne, H. Jhuang, E. Garrote, T. Poggio, and T. Serre, "Hmdb: a large video database for human motion recognition," in *ICCV*, 2011. [14](#)
- [188] J. Carreira, E. Noland, A. Banki-Horvath, C. Hillier, and A. Zisserman, "A short note about kinetics-600," *arXiv*, 2018. [14](#)
- [189] L. Wang, Y. Xiong, Z. Wang, and Y. Qiao, "Towards good practices for very deep two-stream convnets," *arXiv*, 2015. [14](#)
- [190] B. Fernando, H. Bilen, E. Gavves, and S. Gould, "Self-supervised video representation learning with odd-one-out networks," in *CVPR*, 2017. [15](#)
- [191] D. Jayaraman and K. Grauman, "Slow and steady feature analysis: higher order temporal coherence in video," in *CVPR*, 2016. [15](#)
- [192] T. Han, W. Xie, and A. Zisserman, "Video representation learning by dense predictive coding," in *ICCV-W*, 2019. [15](#)
- [193] D. Kim, D. Cho, and I. S. Kweon, "Self-supervised video representation learning with space-time cubic puzzles," in *AAAI*, 2019. [15](#)
- [194] J. Wang, J. Jiao, L. Bao, S. He, Y. Liu, and W. Liu, "Self-supervised spatio-temporal representation learning for videos by predicting motion and appearance statistics," in *CVPR*, 2019. [15](#)
- [195] S. Benaim, A. Ephrat, O. Lang, I. Mosseri, W. T. Freeman, M. Rubinstein, M. Irani, and T. Dekel, "Speednet: Learning the speediness in videos," in *CVPR*, 2020. [15](#)
- [196] S. Jenni, G. Meishvili, and P. Favaro, "Video representation learning by recognizing temporal transformations," in *ECCV*, 2020. [15](#)
- [197] J. Zbontar, L. Jing, I. Misra, Y. LeCun, and S. Deny, "Barlow twins: Self-supervised learning via redundancy reduction," *arXiv*, 2021. [15](#)
- [198] A. Recasens, P. Luc, J.-B. Alayrac, L. Wang, F. Strub, C. Tallec, M. Malinowski, V. Pătrăucean, F. Altché, M. Valko, J.-B. Grill, A. van den Oord, and A. Zisserman, "Broaden your views for self-supervised video learning," in *ICCV*, 2021. [15](#)
- [199] M. Caron, H. Touvron, I. Misra, H. Jégou, J. Mairal, P. Bojanowski, and A. Joulin, "Emerging properties in self-supervised vision transformers," in *ICCV*, 2021. [15](#)
- [200] S. Shen, Z. Dong, J. Ye, L. Ma, Z. Yao, A. Gholami, M. W. Mahoney, and K. Keutzer, "Q-bert: Hessian based ultra low precision quantization of bert," *AAAI CAI*, 2020. [16](#)
- [201] Y. Huang, Y. Cheng, A. Bapna, O. Firat, D. Chen, M. Chen, H. Lee, J. Ngiam, Q. V. Le, Y. Wu, and z. Chen, "Gpipe: Efficient training of giant neural networks using pipeline parallelism," in *NeurIPS*, 2019. [16](#)
- [202] D. So, Q. Le, and C. Liang, "The evolved transformer," in *ICML*, 2019. [16](#)
- [203] S. d'Ascoli, H. Touvron, M. Leavitt, A. Morcos, G. Biroli, and L. Sagun, "Convit: Improving vision transformers with soft convolutional inductive biases," *arXiv*, 2021. [16](#)
- [204] S. Serrano and N. A. Smith, "Is attention interpretable?" in *ACL*, 2019. [16](#)
- [205] S. Jain and B. C. Wallace, "Attention is not explanation," in *NAACL-HLT*, 2019. [16](#)
- [206] S. Wiegrefe and Y. Pinter, "Attention is not not explanation," in *EMNLP-IJCNLP*, 2019. [16](#)
- [207] H. Chefer, S. Gur, and L. Wolf, "Transformer interpretability beyond attention visualization," in *CVPR*, 2021. [16](#)
- [208] S. Abnar and W. H. Zuidema, "Quantifying attention flow in transformers," in *ACL*, 2020. [16](#)
- [209] A. M. Braşoveanu and R. Andonie, "Visualizing transformers for nlp: a brief survey," in *Information Visualisation (IV)*, 2020. [16](#)
- [210] D. Hendrycks, X. Liu, E. Wallace, A. Dziedzic, R. Krishnan, and D. Song, "Pretrained transformers improve out-of-distribution robustness," in *ACL*, 2020. [16](#)
- [211] K. Lu, A. Grover, P. Abbeel, and I. Mordatch, "Pretrained transformers as universal computation engines," *arXiv*, 2021. [16](#)
- [212] C. Zhang, M. Zhang, S. Zhang, D. Jin, Q. Zhou, Z. Cai, H. Zhao, S. Yi, X. Liu, and Z. Liu, "Delving deep into the generalization of vision transformers under distribution shifts," *arXiv*, 2021. [16](#)
- [213] S. Bhojanapalli, A. Chakrabarti, D. Glasner, D. Li, T. Unterthiner, and A. Veit, "Understanding robustness of transformers for image classification," in *ICCV*, 2021. [16](#)
- [214] R. Goyal, S. Ebrahimi Kahou, V. Michalski, J. Materzynska, S. Westphal, H. Kim, V. Haenel, I. Freund, P. Yianilos, M. Mueller-Freitag *et al.*, "The" something something" video database for learning and evaluating visual common sense," in *ICCV*, 2017. [21](#), [23](#), [24](#)
- [215] J. Pennington, R. Socher, and C. D. Manning, "Glove: Global vectors for word representation," in *EMNLP*, 2014. [21](#)
- [216] S. Hershey, S. Chaudhuri, D. P. W. Ellis, J. F. Gemmeke, A. Jansen, R. C. Moore, M. Plakal, D. Platt, R. A. Saurous, B. Seybold, M. Slaney, R. J. Weiss, and K. Wilson, "Cnn architectures for large-scale audio classification," in *ICASSP*, 2017. [21](#)
- [217] Y.-L. Sung, C.-Y. Hong, Y.-C. Hsu, and T.-L. Liu, "Video summarization with anchors and multi-head attention," in *ICIP*, 2020. [22](#)
- [218] A. Prakash, K. Chitta, and A. Geiger, "Multi-modal fusion transformer for end-to-end autonomous driving," in *CVPR*, 2021. [23](#)

– SUPPLEMENTARY MATERIAL –

The supplementary material includes the following: Sec. S1 to provide additional details on dealing with multi-modality in Video Transformers (VTs); Sec. S2 to detail specific trends of VTs for applications other than video classification; and Sec. S3 to complement the performance results from Sec. 4.1.1 in the main paper on two additional video classification datasets: Kinectics-600 [146] and Something-Something v2 [214].

S1 ADDITIONAL DETAILS ON MULTI-MODALITY

Given the widespread use of other modalities in VTs, we deemed it necessary to provide some degree of detail on how these are handled. In particular, we overview how some of the modalities often accompanying video are embedded and also highlight the use of modality embeddings to aid the multi-modal VTs treating each separately.

S1.1 Text and audio embedding

Proper embedding and tokenization is required to the establish coherency among the different inputs, making them spatially and temporally relatable. Also during the embedding, it is common to map the tokens from different modalities to feature representations of the same dimensionality to ease their integration in the later Transformer layers.

Text. When leveraging text (sequences of words) as an additional modality for VTs, the embeddings techniques commonly utilized are GloVe [215] (e.g., [53], [54], [55]), Word2Vec (e.g., [104]) or, directly, the representations provided by a pre-trained BERT [2] (e.g., [65], [70], [71], [104]). Compared to BERT, GloVe and Word2Vec are simpler methods based on, respectively, matrix factorization and shallow neural networks that are trained unsupervisedly based on statistical patterns, such as co-occurrence. The idea behind those is to find a representation of the words that reduce the distance between semantically similar words (e.g., car and bike). **Audio.** The audio modality is typically handled in one of two ways, as a raw audio (i.e., sequence of high-frequency sampled amplitudes) [49], [130]) or, more commonly, as an image of rasterized log-mel spectrograms [54], [64], [97], [104], which is then embedded through a CNN. For instance, VGGish [216] defines a window of 960ms where Fourier features are extracted every 25ms with stride of 10ms encoded in 64 frequency bins, eventually resulting in a spectrograms of 96x64.

S1.2 Modality embeddings

Multi-modal VTs that follow encoder-based fusion schemes incorporate the so-called modality embeddings (e.g., [13], [64], [69], [70], [104]). These are similar to positional embeddings, but signaling the source modality of the tokens in the multi-modal input sequence, so the Transformer can treat them accordingly. These embeddings are learned and summed together with the feature embeddings and the positional embeddings altogether. Exceptionally, there are works that handle this differently. The work of [50] uses separator tokens in a similar fashion as [SEP] in BERT [2], which was thought as a way to indicate the start of a second

sentence, and adapted here to indicate that the following tokens are from a different modality. On a different note, [130] comments on the limitation that all input modalities ought to have the same dimensionality in order to concatenate them. To solve this, the authors concatenated fixed modality embeddings of different sizes for each modality so tokens from all modalities end up having the same dimensionality.

S2 APPLICATION TO OTHER TASKS

While on the main document we outline main trends for VTs applied to video classification, here we delve into trends that are general across tasks first, and then discuss specific trends for a number of different applications.

Encoder-only architectures, which are the most popular for classification, are also utilized for retrieval [69], [71], [104] and summarization [40], [126], [128]. For captioning, instead, encoder-decoder schemes are followed simply because of their autoregressive nature [54], [56], [57]. The latter are also seen for tracking [82], [111], [112], where the decoder augments the search image features by cross-correlating (i.e., attending) to the template features provided by the encoder. Decoder-only models are uncommon across tasks, but examples are found for captioning [101], localization [52], and text-to-video retrieval [51].

Tasks such as captioning, retrieval, and summarization mostly rely on temporal information and found to primarily employ frame-based [14], [69], [126] or clip-based tokenization [50], [104], [128], whereas tasks such as tracking, object detection and segmentation employ patch-based tokenization [82], [119], [122] as it allows maintaining enough spatiotemporal granularity to relate object or smaller regions. Minimal embeddings are tightly related to pure Transformers, which are hardly seen outside classification. Notable exceptions are the works of [60] on video generation or [80] on action anticipation.

Regarding efficient designs, aggregation and restriction strategies are exploited equally often across numerous tasks. Aggregation is found in video classification [12], [48], captioning [14], and retrieval [69], [71], [104]. Restriction is seen also in classification [9], [11] and occasionally in captioning [57], but not in retrieval given almost all works leverage frame embeddings. Weight sharing seems to pay off mostly for big classification models: [71] share the same encoder for different temporal clips, whereas [12] share weights for different local spatiotemporal windows (similar to convolutional layers). Instead, [49] and [64], respectively, share the weights across encoders and their layers dealing with different modalities.

Then, multi-modal approaches are seen mostly for captioning and retrieval, apart from classification. Indeed, all captioning VTs are multi-modal by our definition: their output is text and the input has to be video. Retrieval works are also multi-modal, except for the video-to-video retrieval work of [68]. Amongst modalities considered, audio is not as prominent as text, but still often considered. The works of [54], [56], [101] use it for captioning and [69], [70], [71], [104] for retrieval. In contrast, segmentation, object detection, and summarization were found to be exclusively visual.

Finally, self-supervision has been seen for pre-training big models for classification [11], [49], [130], but also for cap-

tioning [13], [50]. For retrieval it happens to be a core component to bring representations from different videos [68] or modalities together [69], [70], [104].

Importantly, we highlight that many VTs using large-scale datasets to pre-train without supervision (before either fine-tuning for downstream supervised tasks [14], [49], [64], [97], [104] or training a classifier on the learned features [13], [50]) could be regarded as general representation learning. However, task-wise we grouped them with other works performing one of the tasks that follow next.

S2.1 Action detection/localization

Transformers have been applied to both temporal [52], [53] and spatiotemporal action localization [10], [81], [117]. Encoder modules are generally used to fuse information among modalities [53], frames in a sequence [117], or features of CNN-based detections with contextual cues [10], [81]. In contrast, [52] disregard Transformer encoders, entirely relying on a 3D CNN for modeling input clips and on a DETR inspired VT for decoding the decoding of temporal action segments. Except for the single-stage localization of [117], the rest of works rely on sophisticated backbones, either object detectors [10], [81] or temporal boundary regressors to better guide the temporal localization of actions [52], [53].

S2.2 Retrieval

All works solving the task of video retrieval leverage separate streams for each modality and learn a common representation space for both (video and textual caption) using contrastive losses. Some use an encoder fusion method to aggregate multiple visual experts [69], [104], [108] while others propose using hierarchical methods by either enforcing a contrastive loss at both low and high level of features [70], [71]. A subset of works [14], [51], [69], [139] leverage secondary losses to aid the main contrastive objective. The video-to-video retrieval work of [68] is interestingly the only VT to use a supervised contrastive loss.

S2.3 Tracking

Most work in tracking focus on discriminative tracking [82], [111], [112], [113] by employing a Transformer to spatially relate the tracked object to its surroundings, effectively leveraging the global attention to discriminate between tracked object and background. Since the Transformer relies on an accurate representation, the template feature used for discrimination is progressively updated with a moving average [111], [113]. Alternatively the Transformer can be used to attend objects which interact with the tracked object and use that to infer tracking and predict movements of occluded actors and/or objects [63].

S2.4 Captioning

Works that focus on captioning leverage either visual [57], [58], [59] information or are complemented with audio and text [54], [56]. The main trend is to exploit temporal interactions to isolate and pinpoint smaller events in the input to produce dense captions [54], [56], [57], [59]. These

events are often localized with the same encoder network by performing two passes. The event proposals can then be used to mask the SA operation in the second pass [57], [59] or cropped into clips before inputting the video again [54], helping the Transformer to focus on a select set of input tokens. In the case of [56] the event proposals are produced by an independent LSTM instead. In [58], the different video clips are processed by a recurrent VT that autoregressively produces consecutive sentences to form a complete paragraph.

S2.5 Object Detection

VTs in object detection leverage Transformers' global attention to refine feature representations before applying transposed convolutions and following detection heads [92], [119], [173]. However due to the coarse representation, smaller objects are negatively affected by this global attention. The work of [119] partially alleviates this with multi-scale parallel Transformer layers. Spatial Transformers can be employed to effectively attend to relevant fine-grained and global information in dense/noisy point clouds [42].

S2.6 Segmentation

Most work in segmentation leverage temporal relations to refine intermediate feature representations [88], [122], [123]. Most notably, [122] leverages the Transformers ability to view the entire sequence, to include an auxiliary loss where representations of individuals are matched temporally, effectively teaching the network to implicitly track objects and leverage temporal fine-grained information. Alternatively, [124] leverages a novel word-visual attention mechanism allowing a textual query to attend to specific content in multiple spatial scales and perform segmentation based on said query.

S2.7 Summarization

Few works have used Transformers for the task of video summarization by predicting frame-wise importance scores. We find two key trends when solving this task through VTs: the use of RNNs as an initial step [126], [217] and using individual frames to attend to aggregated subsets of the video either from a GRU [217] or by using a masked Transformer [128].

S2.8 Low level tasks

Given the high dimensionality of video data, video generation tasks are quite challenging, and not many video Transformers try to address them. In particular, [60], [61] tackle future frame prediction, [62] generates grayscale video from event-based videos and [114], [115] perform video inpainting. Most of these propose to embed a Transformer within some type of convolutional auto-encoder to evolve representations between encoder and decoder [62], [114], [115]. The only exception is [60], which performs local attention and generate video autoregressively one pixel channel at a time. Interestingly, [115] outperforms [114] in all tested benchmarks for inpainting by using an overlapping patch tokenization strategy.

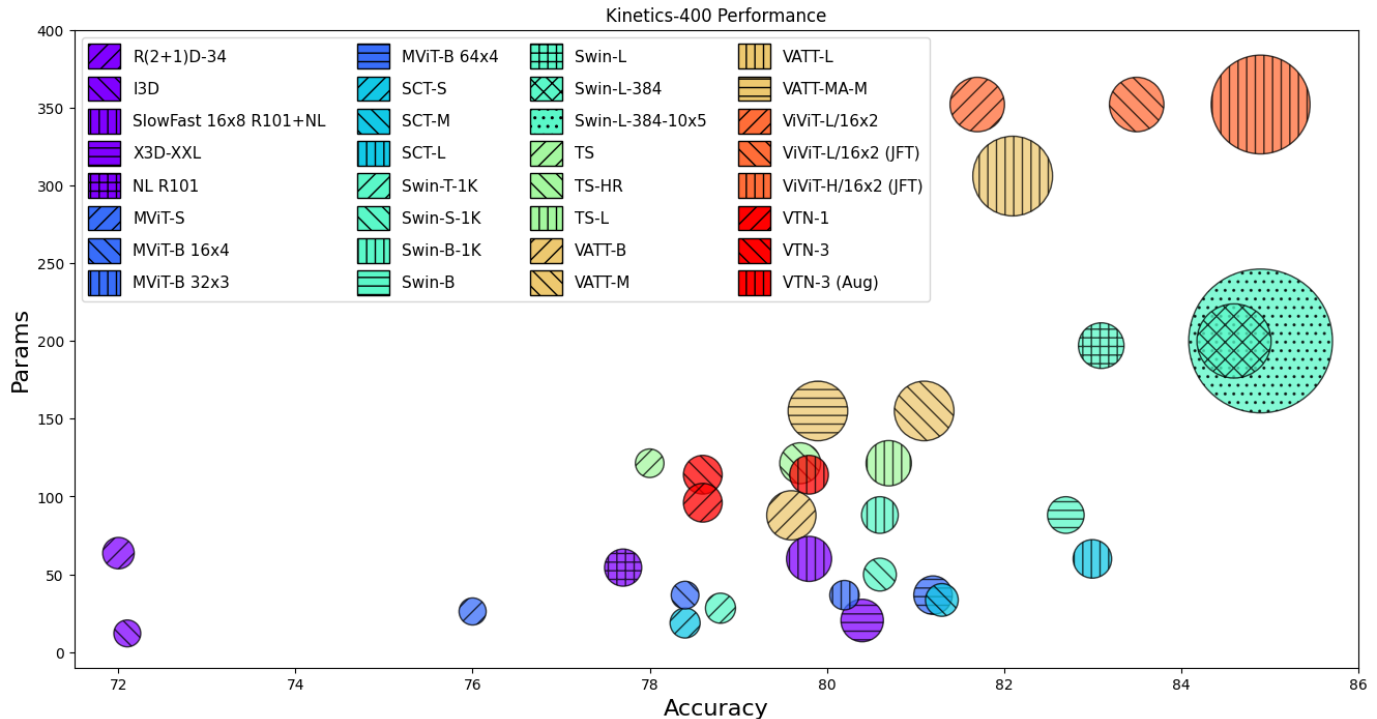


Fig. S1. Performance comparison for video classification methods on Kinetics-400 [146], where the size of the circles represents the TFLOPs, taking account the total number of views. In particular, we illustrate the different variants of the VTs (i.e., MViT [48], SCT [90], VideoSwin [12], TS [9], VATT [49], ViViT [11], and VTN [99]) in different colors and fill patterns, as well as 3D-CNN based models (i.e., R(2+1)D-34 [94], I3D [87], SlowFast 16x8 R101+NL [83], X3D-XXL [185], NL R101 [15]) in purple. Best viewed in color. See Tab. S1 for extra details and results on different datasets.

S2.9 Other tasks

Transformers have also been applied for action anticipation [67], [80], sign-language translation [78], [136], visual-question answering [55], [138], autonomous driving [218], robot navigation [134], visual-language navigation [66], personality recognition [142], lip reading [137], dynamic scene graph generation [131], and multimedia recommendation [141]. As not many video Transformers have tackled this, it is too early to ascertain specific trends, so we simply list them here for completeness.

S3 ADDITIONAL PERFORMANCE RESULTS

In the main paper, we discussed in detail the performance of several Transformer-based and 3D-CNN models for the task of video classification on Kinetics-400 (K400) Sec. 4.1.1. In addition, here we report the results of the same models on Kinetics-600 (K600) [146] and Something-Something v2 [214]. These are illustrated in Tab. S1, where we additionally report the total number of TFLOPs (“Total TF”), that takes into account the number of views utilized during inference. In Fig. S1 we show that same information but in a graphical way for ease of comparing the multiple models. All in all, the results and trends we observe across the other datasets are consistent with the results on K400 already discussed in the main paper.

	Ref.	Name	Input	$(v_t \times v_s)$	TF	Total TF	MP	Pretrain	K400		K600		SSv2 (top-1)		
									Top1	Top5	Top1	Top5	IN-1K	K400	K600
3D-CNNs	[94]	R(2+1)D-34	32 x 112 ²	10 x 1	0.152	1.52	63.6	-	72.0	90.0	-	-	-	-	-
	[87]	I3D	64 x 224 ²	-	0.108	-	12.0	IN-1K	72.1	90.3	-	-	-	-	-
	[83]	SlowFast 16x8 R101+NL	16 x 256 ²	10 x 3	0.234	7.02	59.9	-	79.8	93.9	81.8	95.1	-	-	-
	[185]	X3D-XXL	16 x 312 ²	10 x 3	0.194	5.82	20.3	-	80.4	94.6	-	-	-	-	-
	[15]	NL R101	128 x 224 ²	10 x 1	0.359	3.59	54.3	IN-1K	77.7	93.3	-	-	-	-	-
Transformers	[48]	MViT-S	16 x 224 ²	5 x 1	0.03	0.16	26.1	-	76.0	92.1	-	-	-	-	-
		MViT-B 16x4	16 x 224 ²	5 x 1	0.07	0.35	36.6	-	78.4	93.5	82.1	95.7	-	64.7	66.2
		MViT-B 32x3	32 x 224 ²	5 x 1	0.17	0.85	36.6	-	80.2	94.4	83.4	96.3	-	67.1	67.8
		MViT-B 64x4	64 x 224 ²	3 x 3	0.46	4.10	36.6	-	81.2	95.1	-	-	-	67.7	-
	[90]	SCT-S	24 x 224 ²	4 x 3	0.09	1.06	18.7	IN-21K	78.4	93.8	77.5	93.1	-	-	-
		SCT-M	24 x 224 ²	4 x 3	0.16	1.95	33.5	IN-21K	81.3	94.5	81.7	95.5	-	-	-
		SCT-L	24 x 224 ²	4 x 3	0.34	4.11	59.9	IN-21K	83.0	95.4	84.3	96.3	-	-	68.1
	[12]	Swin-T-1K	32 x 224 ²	4 x 3	0.09	1.06	28.2	IN-1K	78.8	93.6	-	-	-	-	-
		Swin-S-1K	32 x 224 ²	4 x 3	0.17	1.99	49.8	IN-1K	80.6	94.5	-	-	-	-	-
		Swin-B-1K	32 x 224 ²	4 x 3	0.28	3.38	88.1	IN-1K	80.6	94.6	-	-	-	-	-
		Swin-B	32 x 224 ²	4 x 3	0.28	3.38	88.1	IN-21K	82.7	95.5	84.0	96.5	-	69.6	-
		Swin-L	32 x 224 ²	4 x 3	0.60	7.25	197.0	IN-21K	83.1	95.9	-	-	-	-	-
		Swin-L-384	32 x 384 ²	4 x 3	2.11	25.28	200.0	IN-21K	84.6	96.5	85.9	97.1	-	-	-
		Swin-L-384-10x5	32 x 384 ²	10 x 5	2.11	105.35	200.0	IN-21K	84.9	96.7	86.1	97.3	-	-	-
	[9]	TS	8 x 224 ²	1 x 3	0.20	0.59	121.4	IN-21K	78.0	93.7	79.1	94.4	59.5	-	-
		TS-HR	16 x 448 ²	1 x 3	1.70	5.11	121.4	IN-21K	79.7	94.4	81.8	95.8	62.2	-	-
		TS-L	96 x 224 ²	1 x 3	2.38	7.14	121.4	IN-21K	80.7	94.7	82.2	95.6	62.4	-	-
	[49]	VATT-B	32 x 320 ²	4 x 3	0.76	9.09	87.9	AS + H100M*	79.6	94.9	80.5	95.5	-	-	-
		VATT-M	32 x 320 ²	4 x 3	1.25	15.02	155.0	AS + H100M*	81.1	95.6	82.4	96.1	-	-	-
		VATT-L	32 x 320 ²	4 x 3	2.48	29.80	306.0	AS + H100M*	82.1	95.5	83.6	96.6	-	-	-
		VATT-MA-M	32 x 320 ²	4 x 3	1.25	15.02	155.0	AS + H100M*	79.9	94.9	80.8	95.5	-	-	-
	[11]	ViViT-L/16x2	32 x 224 ²	1 x 3	3.98	11.94	352.0	IN-21K	81.7	93.8	82.9	94.6	65.9	-	-
		ViViT-L/16x2 (JFT)	32 x 224 ²	1 x 3	3.98	11.94	352.0	JFT	83.5	94.3	84.3	94.9	-	-	-
		ViViT-H/16x2 (JFT)	32 x 224 ²	4 x 3	3.98	47.77	352.0	JFT	84.9	95.8	85.8	96.5	-	-	-
[99]	VTN-1	250 x 224 ²	1 x 1	4.21	4.21	96.0	IN-21K	78.6	93.4	-	-	-	-	-	
	VTN-3	250 x 224 ²	1 x 1	4.21	4.21	114.0	IN-21K	78.6	93.7	-	-	-	-	-	
	VTN-3 (Aug)	250 x 224 ²	1 x 1	4.21	4.21	114.0	IN-21K	79.8	94.2	-	-	-	-	-	

* Only a subset of HowTo100M (H100M) [148] used for training.

TABLE S1

Classification accuracy on Kinetics-400 (Top1 / Top5) and Kinetics-600 (Top1 / Top5) [146], and Something-Something v2 [214] (Top1) after pre-training on ImageNet-1K or either K400 or K600. "Input" = number of frames x spatial resolution², "TF" = TFLOPs/view, v_t = number of temporal clips, v_s = number of spatial crops, "MP." = millions of parameters.